University of BRISTOL

Department of Computer Science

Porting and optimising the Isca climate model on Intel and ARM processors

George William Lancaster

0000064327

Declaration:

This dissertation is submitted to the University of Bristol in accordance with the requirements of the degree of Master of Science in the Faculty of Engineering. It has not been submitted for any other degree or diploma of any examining body. Except where specifically acknowledged, it is all the work of the Author.

George William Lancaster, September 2019

Climate models use systems of dynamical equations to simulate the changes in global atmospheric behaviour over time. They are computationally demanding and sometimes require many model years of simulation before significant scientific phenomena are captured. To minimise runtimes they are often run in parallel on modern many-core systems, using distributed and shared-memory programming techniques. Isca is an example of one such model, used by the Bristol Research Initiative for the Dynamic Global Environment (BRIDGE) [1].

Many scientific codes are bound by memory-bandwidth. The Cavium ThunderX2 is a new server processor based on the ARMv8 architecture. The recent release of the processor has prompted a wave of research to evaluate its performance [2, 3]. Due to the high memory-bandwidth of the processor, it has seen success when running climate modelling codes such as Isca, and is one of four high performance processors used in this research project.

The main focus of this thesis was to port and optimise Isca on multiple supercomputer clusters, with the aim of presenting an extensive performance analysis of the model. This has allowed for suitable optimisations to be identified, implemented and tested, with successful optimisations integrated back into the codebase. Optimisations include using the Fastest Fourier Transform in the West (FFTW) library to replace a 38-year-old bespoke Fast Fourier Transform. The FFTW library has been specifically designed to utilise the wide vector registers on modern processors and adapts to the hardware on which it is run. Additionally, the model has been compiled to use single-precision floating point numbers by default. When used together, both optimisations provide a performance improvement of up to 1.78× the unmodified code.

This project has successfully provided ports of Isca to four supercomputers, making over 14,000 additional cores available for climate research at the University of Bristol. Additionally, the BRIDGE research group at the University of Bristol has purchased a dedicated £10,000 compute node for the BluePebble supercomputer as a direct result of the work presented in this thesis.

This document is structured into three parts:

Introduction and background Part I introduces the topics discussed throughout this thesis, including high performance computing, climate models and parallelisation infrastructure. Benchmarks of the Sandy Bridge, Broadwell, Skylake and ThunderX2 processors are included, as well as an introduction to various other application benchmarking metrics.

Benchmarking, performance analysis and optimisation Part II details the benchmarking and characterisation of Isca on four different server processors to discover its performance-limiting factors. These include a severe load-balancing issue as well as a number of other minor performance bottlenecks. The two optimisations made to Isca are assessed and evaluated against the unmodified model.

Reflection, critical evaluation and conclusion Part III assesses the outcomes of the project against the intended aims and objectives. There is a discussion of the limitations of the work presented and a reflection of the challenges encountered throughout the project, and how they were overcome.

Acknowledgements

Contents

List of Figures

List of Tables

List of Abbreviations

AVX Advanced Vector Extensions. 8, 14–16, 20, 39, 45

BCP3 BlueCrystal phase 3. 3, 15, 30, 36, 37, 47, 63

BCP4 BlueCrystal phase 4. 3, 4, 15, 25, 29, 30, 45, 47

BP BluePebble. 3, 15, 16, 24, 30, 36, 47

CCE Cray Compiling Environment. 23, 24, 37, 38, 60

CCPG Computational Cost per Grid Point per Time Step. 20, 21, 39, 40

DFT Discrete Fourier Transform. 7, 8, 48

EPSRC Engineering and Physical Sciences Research Council. 5, 16

FFT Fast Fourier Transform. 4, 7, 8, 10, 44–50, 54, 63

FFTW Fastest Fourier Transform in the West. 4, 7, 8, 25, 47–50, 53, 54, 63

FLOPS Floating Point Operations. 18, 21

FMS Flexible Modelling System. 5, 14, 43, 60, 63

GCC GNU Compiler Collection. 22, 24, 31, 37, 38, 46, 57, 60

GCM Global Circulation Model. 5, 6, 29

HPC High Performance Computing. 2–4, 7, 16, 41, 60

HPLinpack High Performance Linpack. 18–20

ICC Intel Compiler Collection. 23, 24, 31, 37, 38, 46

IDFT Inverse Discrete Fourier Transform. 7, 48

MIMD Multiple Instruction Multiple Data. 13, 21, 63

MKMF MakeMakeFile. 22

MPI Message Passing Interface. 5, 11, 22, 23, 31, 40–42, 52, 54, 62, 63

NetCDF Network Common Data Form. 5, 11, 23, 25, 26

PBS Portable Batch System. 4, 24, 30, 61

SIMD Single Instruction Multiple Data. 13, 14, 16, 28, 31, 38, 39, 43, 45–47, 50, 52, 55, 57

SVE Scalable Vector Extensions. 16, 55

ULP Units of Last Place. 25, 26

Part I

Introduction and Background

CHAPTER 1

Introduction

1.1 High Performance Computing

High Performance Computing (HPC) is an interdisciplinary field of computer science that uses distributed supercomputers to solve complex problems across many domains. In academia, HPC is synonymous with scientific computing and has applications including drug discovery, artificial intelligence and the simulation of the natural world [4, 5, 6]. In order to exploit the performance offered by distributed hardware, scientific codes must be written to run in parallel using distributed-memory programming techniques [7]. However, there is often a cost associated with the utilisation of additional compute resources, as more time is spent on communication between processor cores.

Supercomputers are composed of many compute nodes, each containing a number of high performance server microprocessors [8, 9]. The arms race between vendors of consumer hardware is driven by developments in the server market, and as such, the latest features available to modern processors are often demonstrated in server machines. Many scientific applications are based on legacy code that is rigorously tested and well understood. Rewriting such programs can be both expensive and time consuming, and in many cases there is no guarantee that the code can be improved. Recent improvements to computational hardware have been notoriously difficult to utilise, and therefore many scientific codes remain unoptimised throughout many years of service.

1.2 Climate modelling

Climate models are an important tool for understanding the global environmental behaviour of Earth and other celestial bodies. They provide a medium for the reproduction of past, present and future meteorological events, and offer insight into previously unobservable phenomena. However, complex simulations can take thousands of hours to return substantial results, limiting the speed of research. The demand for additional compute resources in academia is unrelenting, with queue times on some University of Bristol machines lasting upwards of several days. Many academics have tight deadlines to meet requirements for both funding and publication, and therefore the procurement of further resources is of the utmost importance.

Climate models are governed by numerous parameters, many of which are idealised and do not correspond to real-world processes. Selecting values for such parameters is non-trivial, and is usually achieved using a brute-force approach known as a 'perturbed physics ensemble' that involves running many simulations using a range of parameter configurations [10]. This strains supercomputer resources further, as jobs are typically submitted in large batches with each job taking many cpu-hours to complete.

1.3 Aims and Objectives

This research project aims to present a comprehensive performance analysis of the Isca climate model on both Intel and Arm processors. For the project to be successful, the model must be ported to three HPC systems and optimised with the goal of reducing the model's runtime. To meet this aim, the following objectives have been identified:

Port Isca to three new HPC systems Isca must be ported from the BlueCrystal phase 4 (BCP4) supercomputer to three other HPC systems: BlueCrystal phase 3 (BCP3), BluePebble (BP) and Isambard. BCP3, BCP4 and BP are based on the Intel x86-64 architecture, and Isambard is based on Arm's ARMv8 instruction set architecture. Isca is dependant on several libraries that are not yet available on the Arm machine. Identifying and porting these libraries comprises a significant part of the project.

Characterisation of the Isca code Isca must be benchmarked and profiled using a variety of performance analysis tools to identify the code's limitations. The resulting data must be used to plan at least two performance optimisations. Additionally, runtimes on each system must be measured to determine how the total program runtime varies as a function of model resolution and number of processor cores.

Optimisation of Isca All identified performance optimisations must be implemented to a high standard. To allow for integration, all code modifications must follow the same style and naming conventions as found in the rest of the codebase.

Analysis of Optimisations To ensure that the optimisations improve the model's performance, the optimised code must be recharacterised and compared to the unoptimised model. To be deemed successful, an optimisation must deliver a consistent improvement to performance. Additionally, it must generate the same output as the unoptimised code, verifying that the application logic is unchanged. It is also important to measure the performance portability of the optimisations, as a performance improvement on one machine may not carry over to another.

1.4 Hypotheses

This project investigates three hypotheses:

Hypothesis 1: Isca is not making use of the latest hardware features on modern processors, and this is limiting its performance.

Hypothesis 2: Some of the hardware-limiting factors of Isca can be addressed to improve the overall performance of the code.

Hypothesis 3: The ThunderX2 processors will not perform as well as the Intel processors.

1.5 Contributions

The work presented in this thesis makes the following contributions to the Isca codebase, and the wider area of high performance computing:

Provision of additional compute resources Prior to this research project, University of Bristol researchers could only access Isca on BCP4, one of five supercomputers available to the university. By providing ports of Isca to other systems, over 14,000 additional cores have

been made available for climate research. Not only has this eased congestion on BCP4, it also makes Isca more accessible to other research groups outside of the university. Additionally, the Bristol Research Initiative for the Dynamic Global Environment (BRIDGE) at the Univerisity of Bristol has purchased a dedicated £10,000 compute node for the BluePebble supercomputer as a direct result of the work presented in this thesis.

Comprehensive performance analysis A scaling study has been performed, which shows how the total program runtime varies as a function of model grid resolution and number of processor cores. This is important for researchers as it allows them to make an informed decision when selecting the number of cores to run different model resolutions. Additionally, a number of performance bottlenecks have been identified, which contributes to the understanding of the limitations of the code.

Optimisation of legacy code for modern hardware This research project demonstrates that Isca does not utilise many of the new hardware features available to modern processors. Specifically, there are many loops found within a bespoke Fast Fourier Transform (FFT) that do not make use of vector instructions. As a result of this observation, this FFT has been replaced with a call to the Fastest Fourier Transform in the West (FFTW) library, producing a code speedup of up to $1.17\times$ the original implementation.

Optimisation of single-precision floating points numbers By halving the default precision of floating point numbers Isca can better utilise vector registers. This presents a performance speedup of $1.69\times$ the unmodified code, and a speedup of $1.78\times$ when used together with FFTW.

Contribution to hardware development Recent developments in consumer mobile hardware have resulted in a new generation of HPC-optimised Arm processors, which were designed to meet the low-power consumption requirements of exascale computing. This research project provides a comparison of these new processors and the current state-of-the-art Intel processors. This is vital to reduce the cost of components and to drive further innovation. This study is a continuation of previous work by other authors, and provides insight into the performance of the Arm hardware on a widely used scientific code [3].

Contribution to cluster development The BluePebble cluster was still in its beta phase of development throughout this research project. All results collected on this machine have been used to influence important design decisions, including the default stack size limit and default memory limit for jobs submitted using the Portable Batch System (PBS) job scheduler. Additionally, all dependencies required by Isca have been installed as modules using the build configurations defined by this research project, and these are freely available to use by other users of the systems.

Development of the Isca codebase All modifications made to the Isca codebase as a result of the work carried out in this project have been integrated back into a public fork of the Github repository in a series of pull requests [11].

Documentation and support to researchers Supporting documents have been written to help researchers compile and run Isca on different machines.

CHAPTER 2

Climate modelling

Software development for scientific applications is a multidisciplinary task, and requires knowledge of both computer programming and the scientific domain for which the software is being developed. Although a comprehensive understanding of the mathematics used to simulate climate is not necessary to understand the work presented in this thesis, some domain knowledge is required. This chapter provides this information, presenting a summary of climate modelling codes, and an extensive overview of the workings of Isca.

2.1 The Isca climate model

Isca is an open-source framework for the modelling of the global circulation of planetary atmospheres. It was developed over four years by the climatology research group at the University of Exeter, with version 1 of the model released in 2017 [1]. The development of Isca was funded by the Natural Environment Research Council, the Engineering and Physical Sciences Research Council (EPSRC) and the UK Met Office [1].

The main goal for Isca is to provide a user-configurable climate model, that allows for the simulation of both simple and complex scenarios including those vastly different from Earth. The model has been used to provide evidence for numerous peer-reviewed publications, including the study of monsoons, tidally-locked planets and variations in the seasons [12, 13, 14].

The model itself comprises over 260,000 significant lines of code, and is written primarily in Fortran with some calls to ANSI C, and a Python interface for usability. Isca can be compiled and run on any system with Network Common Data Form (NetCDF) and Message Passing Interface (MPI) libraries, although a supercomputer is required for anything more than simple experimentation [1].

Considering its growing use as an academic research tool, it is of the utmost importance that Isca is portable to a wide variety of computer architectures, and maintains a degree of performance portability. This will allow for the model to be used for research at other institutions and will drive future development for Isca's global userbase.

2.1.1 Global Circulation Model

Although Isca is a new model, much of the code responsible for atmospheric simulation has been adapted from the twenty-one-year-old Flexible Modelling System (FMS), on which many modern climate models have been developed [15, 16, 17]. The FMS is a Global Circulation Model (GCM), and handles aspects of simulation including parallelisation, input and output, data exchange between model grids and the orchestration of time stepping [18].

GCMs simulate the changes in global climate behaviour over time using the set of primitive dynamical equations of motion and state, first described by Vilhelm Bjerknes in the early 20th century [19, 20, 21]. These equations include the hydrodynamic state equation, mass conservation, and thermal energy equations, which govern the distribution of energy in the atmosphere [1, 20]. In theory, these equations are applied in a continuous domain on the whole real line,

however this is not possible to do in simulation due to the restrictions imposed by finite memory resources. To bypass this issue, GCMs decompose the problem domain using a grid-point or spectral representation.

2.1.2 Domain decomposition

Grid-point models discretely represent data, decomposing the problem domain into a three-dimensional structured grid, on which the primitive dynamical equations are applied at each time step of the simulation. Structured grid codes often have high spatial locality in terms of computation, with interactions between cells limited to adjacent neighbours only. This property allows for high scalability, due to various spatial decomposition methods that utilise distributed machines effectively [22].

(a) Grid-point model decomposition   (b) Spectral model decomposition
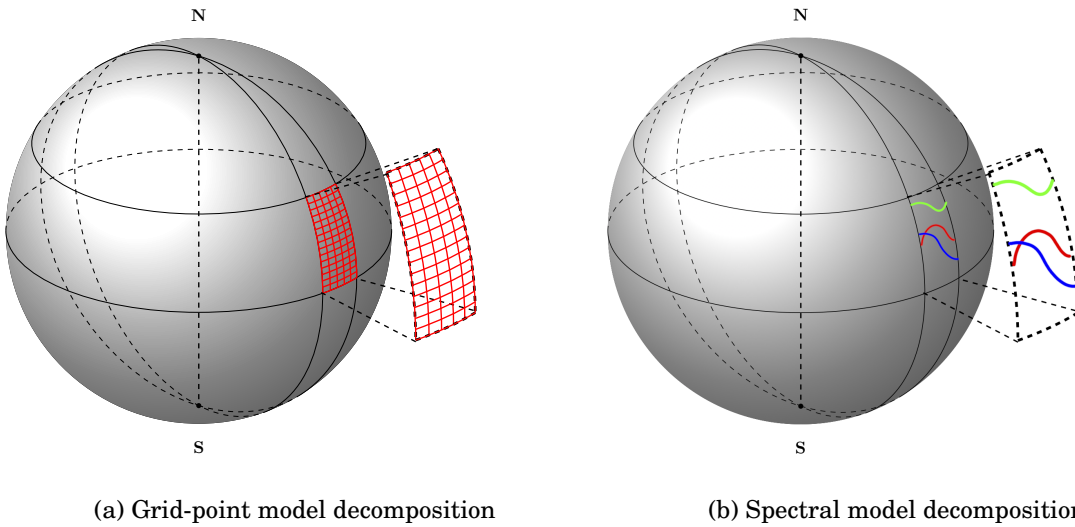
Fig. 2.1: A simplified example of a grid-point and spectral model projected onto the sphere. This example uses just 3 waves, which implies a truncation of T3. Most spectral models use a resolution in excess of 21 waves (T21).

Spectral models represent the spatial variations of atmospheric variables as a finite series of waves at various wavelengths, whereby each wave represents the coefficients of a known function [23]. They are typically used for global climate modelling rather than regional weather prediction as wave functions and spherical harmonics operate over a spherical domain. Because of this, all waves must be periodic so that they wrap around the sphere with the start and finish point using the same value. This places some restrictions on the type of algorithm that can be used, and can add an additional overhead to compute costs as the model must convert the domain into a spatial representation for analysis [24].

Calculating the equations of motion requires solving many partial derivatives in space. Partial derivatives of waves are calculated by summing the derivatives of each basis function, providing an exact result. In contrast, grid-point models must solve partial derivatives by finite differences, and therefore require a higher resolution to provide a comparable degree of accuracy [25].

Resolution

The spatial resolution of a climate model describes the variation in the total amount of data that is used for a given problem size. The resolution of a grid-point model describes the number of

grid cells that the model operates over [26]. A higher cell resolution implies a greater number of cells contained within a grid. Spectral models vary their resolution using a truncation, which refers to the number of waves used to define atmospheric variables [26]. In both cases, there is a trade-off between resolution and model runtime whereby higher resolutions generally result in longer runtimes, but more accurate results.

Climate models have a variable temporal resolution, which refers to the amount of model time that passes in the simulation between calculations. Similarly to spatial resolution, the computational intensity of the simulation is influenced by the granularity of the temporal resolution. Smaller time steps more accurately represent continuous time, but result in longer runtimes.

Both grid-point and spectral models are usually classified as a strong scaling problem, for which the solution time varies with the number of processors for a fixed problem size [27]. Strong scaling is desirable but challenging, as many smaller resolutions are constrained by the number of grid points that can be allocated to a single processor. However, weak scaling can be satisfactory as larger problem sizes can recruit more parallel processing elements.

2.1.3 Fast Fourier Transform

The Isca model uses both grid-point and spectral methods for domain decomposition. A grid-point representation is used for time-stepping, and the physics simulation is applied in the spherical and frequency domains. To convert between these two states, an FFT is used to compute the Discrete Fourier Transform (DFT) of the grid-point representation, and the Inverse Discrete Fourier Transform (IDFT) of the spectral representation. Although the cost of doing this transformation can be relatively high, it often results in a net computational saving, and can produce more accurate data at lower resolutions [28]. Spectral methods are one of the 'seven dwarfs' of HPC popularised by Asanovic *et al.* in 2006, and describe operations applied to data in the frequency domain [7] .

The FFT algorithm is found across many different scientific domains, and as such writing optimised FFT code is a research topic in and of itself [29, 30, 31]. There are multiple highly optimised FFT libraries available, and there are many different approaches to applying the algorithm, each with their own benefits and drawbacks. This research project uses the FFTW library, which was developed by Matteo Frigo and Steven G. Johnson at the Massachusetts Institute of Technology, and first released in 1997 [32].

2.1.4 The Fastest Fourier Transform in the West

FFTW is an implementation of a DFT that adapts to the hardware on which it is run [33]. The library has been written in ANSI C, however it provides interfaces for other programming languages including Fortran. Rather than providing a hand-tuned implementation for all possible hardware configurations, FFTW uses a plan to precompute various sub-arrays based on the shape, size and memory layout of the input data, without requiring the data itself [33]. The planning process yields a plan, which is an executable data structure that returns the DFT of the given input data.

To create a plan optimised for the hardware on which the code is compiled, the planner measures the runtime of many different plan configurations and returns the plan that results in the quickest runtime [33]. The planning process is computationally expensive, however it is only performed once, and the resulting plan can then be reused on different input data of the same dimensions. If many FFTs of the same type are repeatedly called in an application, this generally provides a net performance gain [34].

Plans are created using FFTW's own compiler called genFFT [33]. Whilst the FFTW library itself is written in ANSI C, genFFT is written in Objective Caml, and is used to produce a number of small hard-coded transforms called codelets. Codelets are well-optimised simple straight line programs, which compute the DFT of a small sequence of data. The speed of FFTW is largely accredited to these codelets, which are successively applied to sections of a larger sequence [33].

Although not a requirement of using FFTW, the input data should be contiguous in memory so that vector instructions can be utilised. FFTW version 3.3.8 officially supports Advanced Vector Extensions (AVX) x86 extensions and version 3.3.1 introduced support for the ARM NEON extensions [34]. Version 3.3.8 of the library was chosen for this implementation to target the vector extensions on all hardware configurations used in this research project.

Cooley-Tukey algorithm

Despite FFTW using many different FFT algorithms, the most commonly used is the Cooley-Tukey algorithm. This algorithm was popularised in 1965, however variations of the algorithm have been known as early as 1805 [30, 35]. Proper implementation of the Cooley-Tukey algorithm results in a time complexity of $O(n \log n)$, where n is the number of elements in the DFT. The algorithm is based on the assumption that a DFT of size $N = n_1 \cdot n_2$ can be expressed as a two-dimensional DFT of size $n_1 \times n_2$ [33]. The algorithm itself can be broken into three steps:

1. Perform n_1 DFTs of size n_2;

2. Multiply by some *twiddle factors*, which are a constant complex coefficient that is multiplied by the input data in order to recursively combine small DFTs [36];

3. Perform n_2 DFTs of size n_1.

When presented with this information, it becomes clear why the authors of FFTW decided to use a codelet-based design. An optimal solution to performing the FFT using the Cooley-Tukey algorithm allows for a codelet to calculate the DFT of a data structure of either size n_1 or n_2, and this can be repeated an arbitrary number of times.

One-dimensional real-data DFT

FFTW's real input DFT computes a forward transform Y of a real-type input array X of size N, whereby a forward transform refers to a negative sign before the exponent [33]. The output of this transform will be a complex-type array of size $N/2$, where the kth output corresponds to the frequency k/N. Equation 2.1 shows the forward FFT used by the FFTW library.

$$Y_i = \sum_{j=0}^{N-1} X_j \cdot e^{-2\pi i j \sqrt{-1}/N} \tag{2.1}$$

One-dimensional complex-data DFT

FFTW's complex input DFT computes a backward transform Y of a complex-type input array X of size $N/2$ [33]. The only difference between the forward and backward transform is the sign of the exponent, which is positive for the backward transform. The output of the backward transform is a real-type array of size N. Equation 2.2 shows the backward FFT used by the FFTW library.

$$Y_i = \sum_{j=0}^{N-1} X_j \cdot e^{2\pi i j \sqrt{-1/N}} \tag{2.2}$$

2.2 Software architecture

The Isca codebase is vast, composed of over 290 Fortran90 source files. As it would be impractical to review the entire codebase within the scope of this project, the following section provides a brief introduction to the software architecture of the model.

2.2.1 General overview

Isca is compiled and run using its own Python library, which is used to populate various Bash scripts, Fortran namelists and other miscellaneous files with data entered into multiple dictionaries in a Python script. This was a design decision based on the usability of Python in comparison to the underlying Fortran model, and allows for a lower barrier to entry in terms of technical ability for climate researchers [1].
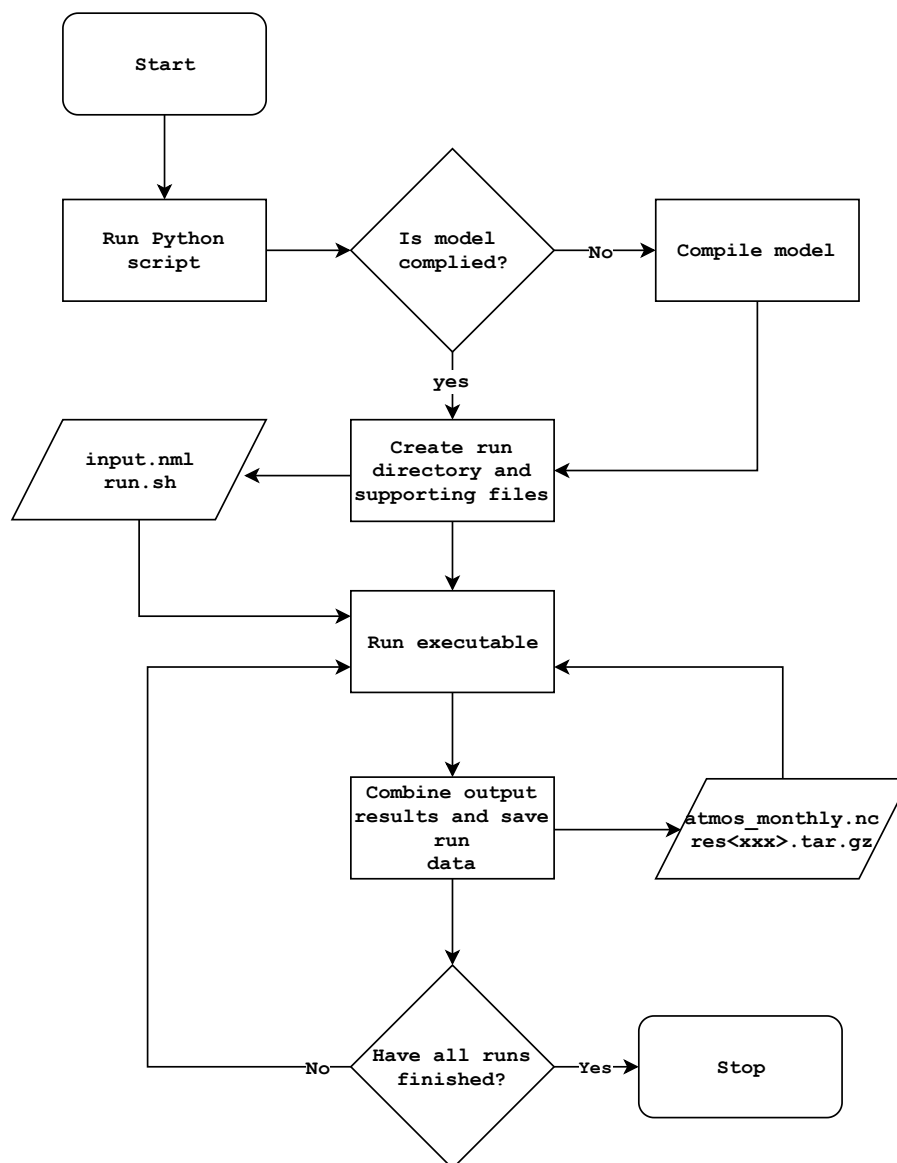
Fig. 2.2: Flowchart illustrating the program logic of Isca when run using it's Python library. The `run.sh` Bash script is repeatedly used to run the Isca executable.

Compiling the model using the Python library produces a single executable that is repeatedly run for a number of epochs defined in a Python script. The length of each epoch is variable, usually lasting for approximately one model month but simplified to 30 model days. When run in parallel the diagnostic output is distributed, which means that each processor writes its own files. Upon completion, the data generated by the previous month's simulation is combined into a single file, and is used as an input to the following month (Figure 2.2). The large number of Python and Bash scripts used to create directories, populate and move supporting files means that the executable cannot be run alone.

The executable itself follows an 'atmosphere integration loop', whereby the state of the atmosphere is computed for a predefined number of time steps. The modularity of Isca allows for the atmosphere to be simulated using a wide range of different techniques and algorithms at varying degrees of complexity and realism, however the most basic atmosphere integration loop is visualised as pseudocode in Listing 2.1.

```
1  Time_next = Time + Time_step
2
3  if(idealized_moist_model) then
4      call idealized_moist_phys(...)
5  else
6      call hs_forcing(...)
7  endif
8
9  call spectral_dynamics(Time, ...)
10
11 if(dry_model) then
12   call compute_pressures_and_heights(x, z, ...)
13 else
14   call compute_pressures_and_heights(x, y, ...)
15 endif
16
17 call spectral_diagnostics(Time_next, ...)
18
19 previous = current
20 current  = future
```

Listing 2.1: Pseudocode for the atmospheric integration loop found in Isca.

The atmosphere integration loop contains many subroutines, however of greatest interest is the `spectral_dynamics` subroutine, which comprises around 95% of the wallclock runtime of any given simulation (Listing 2.1). This subroutine calculates values for various atmospheric variables, which involves communication between processors and a number of FFTs.

Isca's spectral model decomposes the horizontal grid into latitude bands, with each band assigned to a processor. When only two processors are used the grid is split into Southern and Northern Hemispheres [11]. This method of domain decomposition implies that atmospheric variables at the edge cases of each latitudinal band (halo points) must be exchanged with other processors in a process known as a synchronised halo exchange. This allows for parallelism in the Isca model at the cost of an additional overhead incurred by the communication itself. The halo exchange interrupts the computational flow of the program and allows for the exchange of the halo points before the simulation can resume (Figure 2.3).
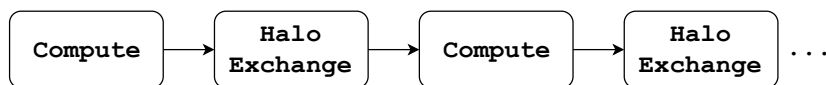
Fig. 2.3: Simple communication pattern. Sections of compute are interrupted by calls to a halo exchange.

2.2.2 Dependencies

Fortran Libraries

Isca relies on MPI for interprocess communication and NetCDF for data storage. These technologies are commonly used in high performance computing and offer interfaces for both the ANSI C and Fortran programming languages [37, 38].

MPI is a standardised, portable interface for interprocess communication that allows for direct data transfer between processors without relying on shared memory [37]. The MPI standard has been implemented by numerous companies and organisations but the most commonly used are OpenMPI, MVAPICH, MPICH, and Intel MPI. All MPI implementations provide the same function calls and interfaces, and can therefore be used interchangeably.

NetCDF is a platform independent binary file type that is commonly used to store and analyse scientific data [38]. NetCDF binary files are self-describing, containing all the necessary information to interpret the data they store. This makes NetCDF files highly portable as a file written on one computer can be read by another without context or specialist tools, aside from the NetCDF library itself. If compiled using an MPI library, NetCDF can provide parallel IO. NetCDF itself is dependant on the HDF5 and zlib libraries, which are used for storage and data compression, respectively. When compiling the NetCDF library or any program that uses it, the same compiler must be used to compile HDF5, zlib, NetCDF and the program itself. One of the advantages of NetCDF is that there are many programs available to visualise the data they store (Figure 2.4).
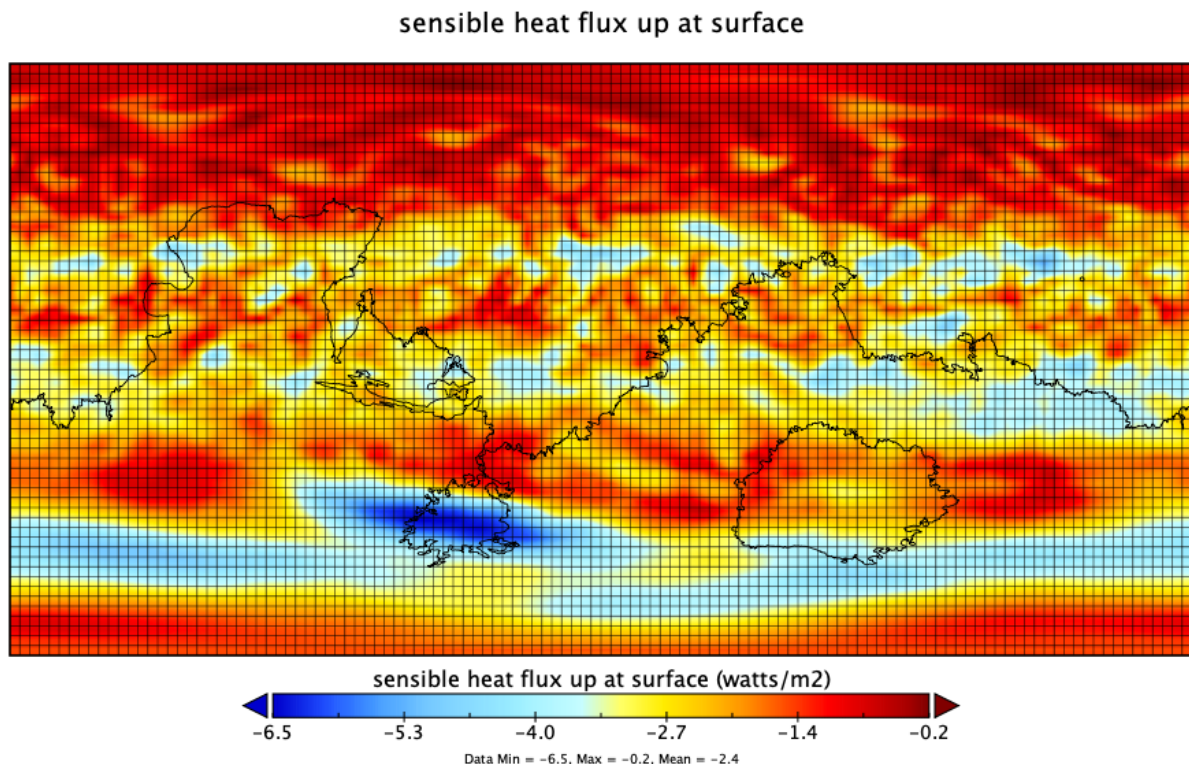
Fig. 2.4: Visualisation of an output of from the Isca model running a Grey-Mars radiation model. The image shows the heat transfer to the Martian surface after 690 days. This visualisation was generated using the Panoply NetCDF data viewer tool [39].

Python libraries

For simplicity, Isca uses a Python interface to create and run different model configurations. To do this, it uses a number of popular Python libraries that are available on many different platforms.

Numpy A mathematics library for Python that allows for the manipulation of N-dimensional arrays [40].

sh A full-featured subprocess replacement for Python that allows for Bash commands to be issued from Python code [41].

Jinja2 A templating language for Python that is typically used in web design. It has been used in Isca to populate a number of Bash script templates with data defined in a series of Python dictionaries [42].

f90nml A Python module and command line tool for reading, writing and modifying Fortran namelist files [43].

CHAPTER 3

HPC hardware and parallel processing

There are many different techniques and processor designs that allow for a program to be run in parallel. This chapter presents a brief but concise overview of two parallel processing techniques that are used by Isca and many other scientific codes, and provides details of the hardware that has been used throughout this research project.

3.1 Parallel processing

To allow for programs to be run in parallel, there are numerous different techniques that can be used. In order to improve the performance of a parallel code, an understanding of these techniques is essential.

3.1.1 Flynn's Taxonomy

Flynn's taxonomy was first proposed by Michael J. Flynn in 1966 to provide a framework with which to place various methods of computation [44]. It defines four unambiguous terms to describe the relationship between data and the technique by which it is processed. The entirety of Flynn's taxonomy is visualised in Figure 3.1, and the following list details the architectures it describes.

Single Instruction Single Data (SISD) refers to the most basic type of processing whereby a single instruction is applied to a single data item stored in memory. Code that uses this processing type is often referred to as scalar or serial.

Single Instruction Multiple Data (SIMD) allows for a single instruction to be applied to multiple data items stored in a contiguous piece of memory. To gain the largest performance benefit from SIMD operations, the multiple data items must be read using a single instruction, and then the same operation must be applied to all items. SIMD processing is often referred to as vectorisation, as the data is processed as a one-dimensional vector.

Multiple Instruction Single Data (MISD) is a rarely used processing technique that applies different operations on identical data. Rather than improving the performance of a program, it is often used for mission critical computations where there is no room for error.

Multiple Instruction Multiple Data (MIMD) is currently the most commonly used parallel processing technique. It describes a machine that contains many asynchronous processors that function independently, and as such, most modern processors can be categorised as MIMD.

Like most scientific codes, Isca uses the SIMD and MIMD approaches to parallelism. As discussed in Section 2.2.2, the model uses the MPI library to split the global domain into latitude bands with each band assigned to a processor. Modern processors also have wider registers in order to apply an instruction-level parallelism technique whereby multiple data items are processed by a single instruction.
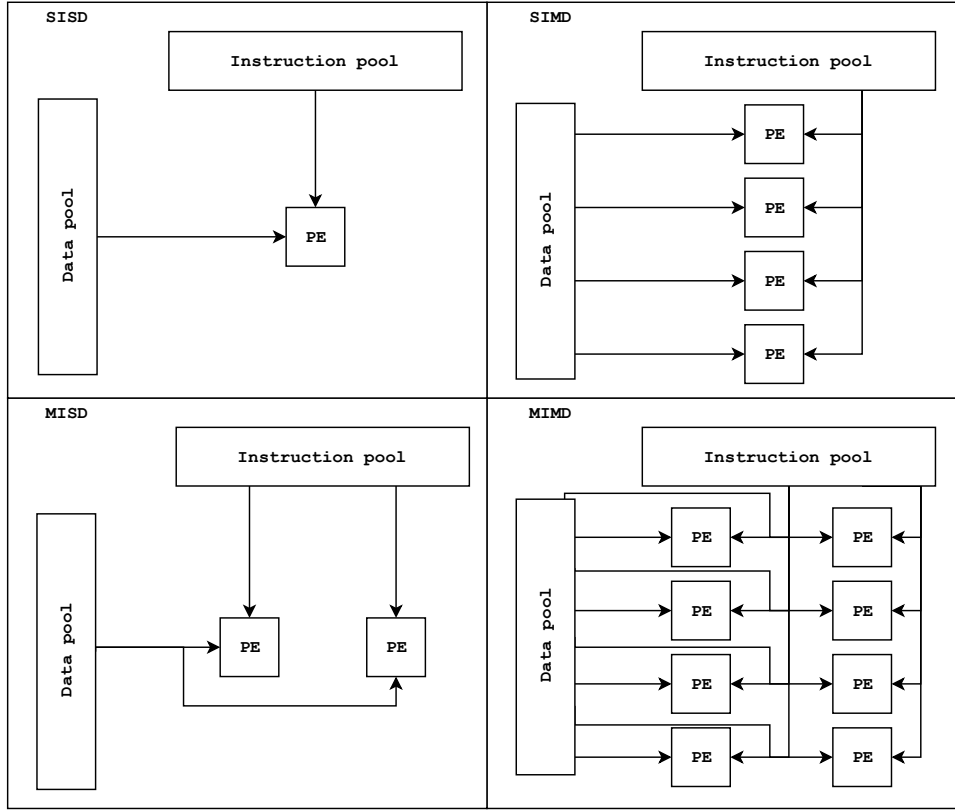
Fig. 3.1: Flynn's taxonomy. Instructions are applied to data by various processing elements (PE) in different ways.

3.1.2 Instruction-level parallelism (SIMD)

From the 1970s to the early 1990s, high performance machines relied heavily on instruction level vector operations to compute in parallel [45]. These machines used vector processors, and performed operations on one-dimensional arrays of data, rather than single data items using a SIMD processor architecture [46]. Many scientific codes from this time were written with this architecture in mind and it is likely that it influenced the design and implementation of the FMS.

Instruction-level parallelism using SIMD is becoming popular once again through the introduction of Intel's AVX. Intel introduced AVX in 2011's Sandy Bridge architecture, AVX-2 in 2013's Haswell architecture and AVX-512 in 2016's Skylake architecture [47, 48]. AVX increased the width of some vector registers to 256 bits, allowing for SIMD operations on four 64-bit elements per clock cycle. In comparison, the AVX-512 instruction set increased vector register width to 512 bits, allowing for SIMD operations on eight 64-bit elements per clock cycle, double that of AVX and AVX-2 [47, 49].

Although AVX-512 has a higher throughput of operations per clock cycle, using wider vector registers results in greater power consumption, which in turn causes the processor to generate more heat. In order to maintain a suitable temperature, Intel processors perform dynamic frequency scaling in order to decrease the clock speed for the duration of the loop using the AVX-512 registers, often resulting in no overall performance gain over AVX-2 [50].

In theory, SIMD can greatly improve the performance of scientific codes as a greater number of operations are applied per clock cycle. However, these performance gains can be difficult to realise in complex applications. Often, compute kernels do not align with the width of SIMD registers, and some kernels have dependencies which prevent a single operation from being applied to many

data items. Therefore wider vector registers often provide only a small performance improvement in production applications.

3.1.3 Distributed-memory parallelism (MIMD)

Processor design has largely evolved since the 1990s when the FMS was under development. During this time, it was not uncommon to have just 1 or 2 processors per compute node [8]. This meant that many parallel codes were reliant on distributed memory programming techniques such as MPI to provide MIMD parallelism. To meet the compute requirements of exascale, compute nodes are now composed of a greater number of processor cores [9, 51]. The definition of 'massively parallel' has shifted over the past 20 years, and codes that were once reliant on message passing can now achieve the same level of scalability whilst utilising only the compute resources of a single node.

As a result of these developments many legacy high performance codes including Isca still use a distributed-memory approach to parallelism. However, many of these codes are now not run in multinode configurations as the cost of communication between compute nodes outweighs the performance gains of increased parallelism.

3.2 HPC clusters

During the course of this research project, Isca has been ported to and run on four different high-performance supercomputers. This section discusses these machines, and the features of their respective processor architectures. A full breakdown of the most important hardware features can be found in Table 3.1. BCP3, BCP4 and BP are all based on the well-established line of x86-64 Intel Xeon processors and Isambard is based on the ARM-v8 Cavium ThunderX2 processor.

Table 3.1: Hardware specifications of the target HPC systems.

Attribute	Intel Xeon (x86-64)			ARMv8
	BCP3	BCP4	BP	Isambard
Processor	E5-2670 v1	E5-2680 v4	Gold 5120	ThunderX2
Codename	Sandy Bridge	Broadwell	Skylake	ThunderX2
Instruction set	AVX	AVX-2	AVX-512	NEON
Clock Speed	2.6 GHz	2.4 GHz	2.2 GHz	2.1 GHz
Cores / Node	2×8	2×14	2×14	2×32
Memory / Node	64 GB	128 GB	256 GB	256 GB
Compute Cores	3,568	14,700	-	10,752
Interconnect	QDR InfiniBand	Omnipath	Ethernet	Cray Aries

3.2.1 BlueCrystal phase 3

BCP3 is primarily intended for smaller jobs that run on a single node, and it is the oldest cluster still in use at the University of Bristol. A single node of BCP3 contains two, eight-core Sandy Bridge Xeon E5-2670 v1 processors, which were the first line of the Intel processors to use AVX, increasing the width of vector registers to 256-bits.

3.2.2 BlueCrystal phase 4

BCP4 has been the University of Bristols main workhorse cluster since 2017. It was designed and configured by OCF in collaboration with Lenovo and is primarily intended for large parallel jobs across multiple nodes. BCP4 now has an established userbase, however the machine is almost at maximum capacity and some longer jobs can spend over a week in the queue before they run.

A compute node of BCP4 contains two fourteen-core Broadwell Xeon E5-2680 v4 processors. They use the AVX-2 instruction set architecture and were introduced by Intel in 2016,

3.2.3 BluePebble

BP is a new Intel-based cluster, managed by the Advanced Computing Research Centre at the University of Bristol. It was created in order to ease congestion on BCP4 by moving some of its heaviest users to their own cluster with dedicated resources. Some members of the meteorological research group at the University of Bristol can be classified as heavy users of BCP4, and have recently purchased a £10,000 dedicated node of BluePebble to conduct their research using Isca.

BP contains two different types of compute node, both using Intel's Skylake architecture. The first contains two twelve-core Xeon Gold 6126 processors and the second contains two fourteen-core Xeon Gold 5120 processors. Both processors make use of AVX-512 instruction set.

3.2.4 Isambard

The GW4 Alliance, which consists of the Universities of Bath, Bristol, Cardiff and Exeter, together with the UK Met Office and Cray Inc have worked together to deliver the Isambard supercomputer, which is the result of a £3m award by the EPSRC [52]. Isambard provides multiple advanced architectures, however the focus of this research project is the Arm-based Cavium ThunderX2 processor, which forms the majority of the machine. Each of Isambard's 168 compute nodes contain 64 ARMv8 cores in a dual-socket configuration [53].

Cavium ThunderX2 Server Microprocessors

Arm primarily designs processors for mobile devices and has only recently produced hardware optimised for HPC systems [3]. Due to the heat generated by high clock rates, modern chip designers are now limited by power consumption. Because of this constraint, the current trend in supercomputer design is to use large shared-memory nodes, that use higher core cores and decreased clock rates [54].

Arm processors have inherently low power consumption as they were originally designed for mobile devices. Because of this, the European Mont-Blanc project began to investigate the potential of the Arm architecture for HPC in 2011 [55]. This project proved to be successful, however the study uncovered some problems with the architecture that have since been addressed during the development of the ThunderX2. ThunderX is a line of 64-bit many-core server microprocessors developed by Cavium as a result of over 8 years of work by the Mont-Blanc project and other contributors. The ThunderX2 was first released in early 2018 as the successor to the ThunderX, and is the first generation of Arm-based server microprocessors intended for high performance computing. Initial studies have found that the ThunderX2 presents as a real alternative to current offerings by vendors of desktop hardware, finding that the processor delivers competitive levels of performance to Intel's line of Xeon processors [2, 3].
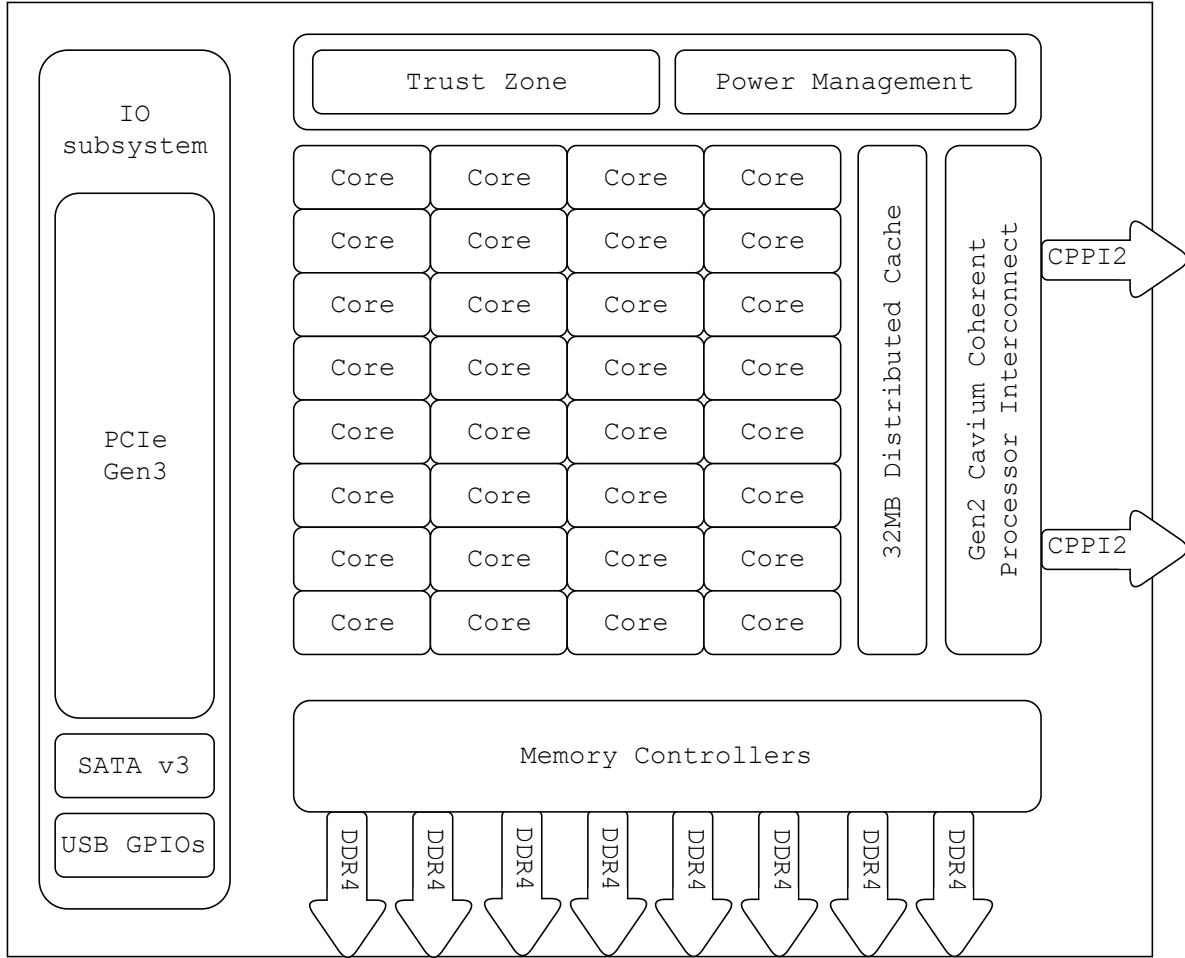
Fig. 3.2: Block diagram of the Cavium ThunderX2 server microprocessor. Diagram redrawn from [53]

The ThunderX2 uses the ARMv8.1 instruction set. This allows for the use of 128-bit NEON SIMD registers, which is Arm's implementation of advanced SIMD extensions. Perhaps the most interesting feature of the ThunderX2 as noted by McIntosh-Smith *et al.* is its eight memory controllers per socket, which have been demonstrated to produce a memory bandwidth in excess of 250GB/s [3]. The layout of the processor is shown in Figure 3.2.

A64FX

To meet the compute requirements of future HPC workloads, Fujitsu has recently announced the next generation of Arm chips in their A64FX processor. The A64FX improves upon the NEON instruction set found in the ThunderX2 by introducing Scalable Vector Extensions (SVE), which allow for a flexible vector register length between 128 and 512 bits so that vector length can reflect the compute requirements of different use cases [56, 57]. These processors have not yet been released, however this thesis provides an estimate of their performance based on the performance of the ThunderX2.

CHAPTER 4

Benchmarking and performance analysis

This chapter is an introduction to benchmarking both hardware and software, and describes some of the techniques and metrics used to benchmark the Isca code.

4.1 Cluster benchmarks

The STREAM TRIAD and High Performance Linpack (HPLinpack) benchmarks have been used respectively to measure the peak memory bandwidth and floating point performance of each node configuration used in this study [59, 62]. This has been done to provide a relative performance overview of each processor architecture and to highlight the differences between them.

4.1.1 STREAM TRIAD

The speed of processors has increased exponentially over the past twenty years as described by Moore's law, which states that the number of transistors in a dense integrated circuit doubles approximately every two years [58]. In comparison, the speed of memory has only marginally improved as manufacturers have historically prioritised memory capacity over speed [59, 60]. The result of this is that many scientific codes are no longer bound by compute, but by the rate at which data can be read from, or stored to memory by the processor. The STREAM memory-bandwidth benchmark was introduced by John McCalpin in 1995 to address the limitations of the benchmarks of the time, and to measure processor performance by its peak memory bandwidth consumption rather than the rate of Floating Point Operations (FLOPS).
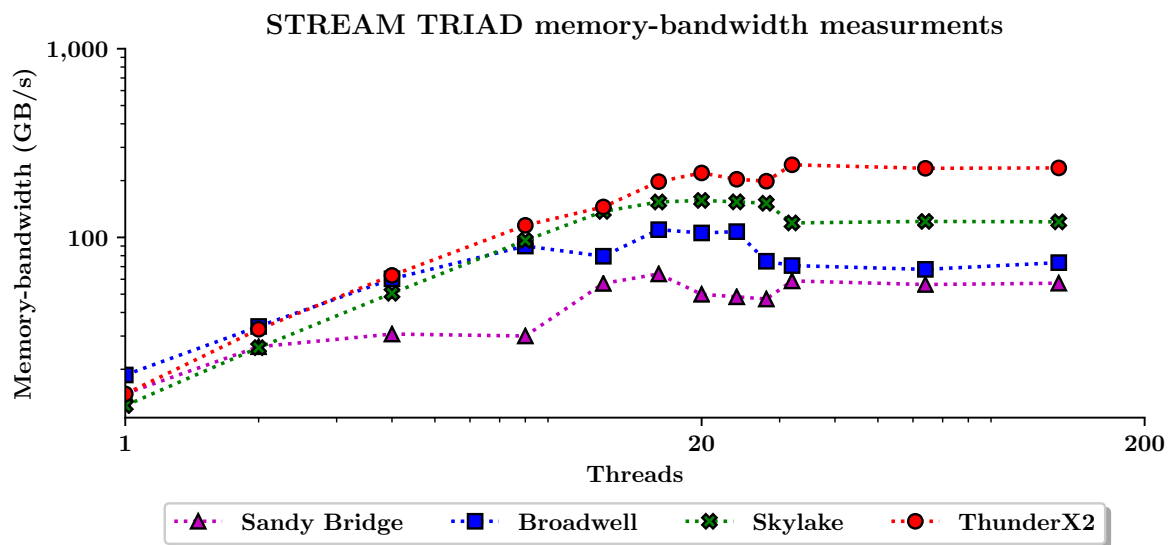
Fig. 4.1: STREAM TRIAD results for all processor architectures that have been used as part of this research project.

As core counts and memory channels continue to grow, it becomes increasingly difficult to measure the memory bandwidth of modern processors, and results can greatly vary depending on the system configuration used to compile and run the benchmark. The results shown in Figure 4.1 were collected using the original STREAM benchmark code [61]. The code was compiled using the Intel compiler with the same flags and environment variables on each cluster with the exception of the ThunderX2 processor, which used the GNU compiler.

The ThunderX2 processor has eight memory controllers per socket, and presents a peak STREAM TRIAD result in excess of 240 GB/s for a dual-socket configuration. In comparison, the Skylake processor provides a result of just 157 GB/s. This observation demonstrates the class leading memory bandwidth of the ThunderX2.

4.1.2 High Performance Linpack

The theoretical peak performance of a compute node can be calculated (Equation 4.1). c denotes the processor speed in GHz, p denotes the number of processor cores, i denotes the number of instructions per clock cycle, and o denotes the number of processors per node.

$$GFLOPS = c \cdot p \cdot i \cdot o \tag{4.1}$$

In general, the theoretical peak performance of a machine is unattainable. The HPLinpack benchmark aims to measure the attainable percentage of peak processor performance by solving a dense system of $n \times n$ linear equations [62]. HPLinpack uses a large number of operations per memory access and so is constrained by the rate of operations rather than memory bandwidth. Figure 4.2 shows the actual performance measured using the HPLinpack benchmark compared to the peak theoretical machine performance calculated using Equation 4.1.
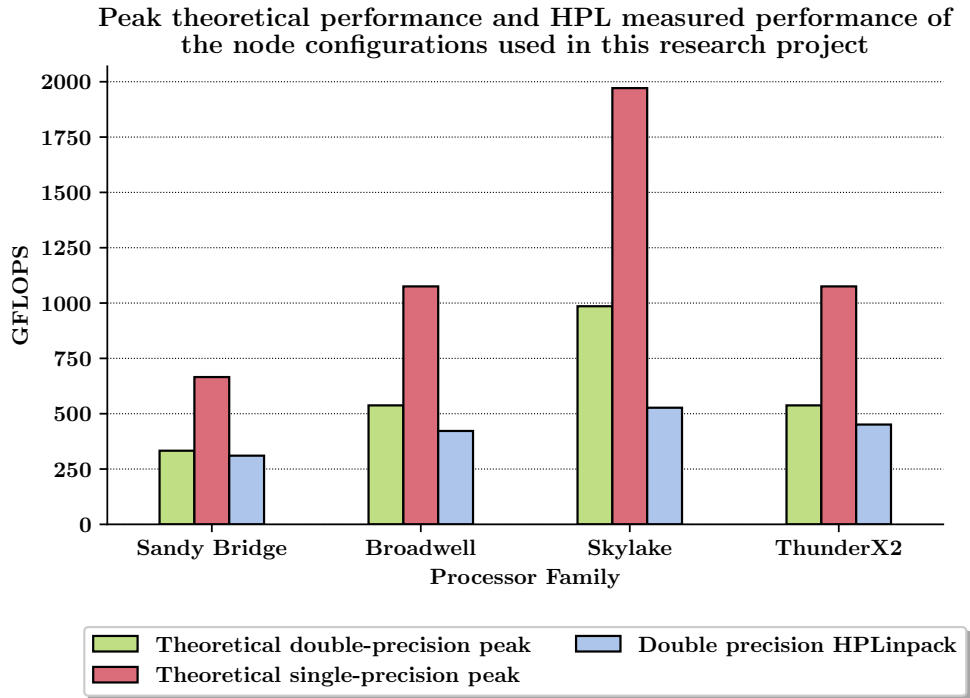
Fig. 4.2: Comparison of the theoretical peak machine performance against the performance measured by HPLinpack.

Although the HPLinpack measured performance is much less than the theoretical peak performance, it is approximately proportional to the theoretical peak. This is confirmation that this benchmark is limited by the rate of operations as if it were constrained by memory-bandwidth, it would be expected that the ThunderX2 would outperform the Skylake processor.

The performance measured using the HPLinpack benchmark is less than the theoretical performance in all cases. The large theoretical peak performance of the Skylake processor is attributed to its wide 512-bit vector registers, which can process 16 double-precision floating point numbers with a single instruction. The signifcantly smaller actual performance measurement is because the processor can only use AVX-512 at a reduced clock rate, and therefore the compilers performance model rarely opts to use these registers.

4.2 Application benchmarking

Floating point performance and memory bandwidth are usually measured using synthetic benchmarks such as the STREAM and HPLinpack benchmarks, and may not provide the best metrics for a complex code like Isca. Although the model is computationally demanding there is also a large overhead cost incurred by communication. This includes tasks such as reading and writing files, the movement of data into contiguous memory and the transmission of data between processors. For this reason, the model can only be expected to achieve a fraction of the theoretical peak memory bandwidth and floating point performance reported in the previous section. Therefore, the following performance metrics have been defined, and are used throughout this study.

4.2.1 Performance metrics

Wallclock runtime

Wallclock runtime refers to the total amount of real time that has passed from the start of the program to the end. In this study, wallclock runtime has been reported in seconds. Used alone, this metric does not provide a basis for comparison between other configurations and therefore three other metrics have also been used.

Speedup

Speedup is a measure of relative performance between two solutions for the same problem. For the metric reported in this study, this is the number of times faster the code ran than some other given benchmark, typically the serial runtime. The speedup S of a code can be calculated given two runtimes R_1 and R_2 using the formula in Equation 4.2, whereby R_1 is $S\times$ faster than R_2 [63].

$$S = \frac{R_1}{R_2} \tag{4.2}$$

Cost per gridpoint

Other studies that have benchmarked parallel climate codes have used the Computational Cost per Grid Point per Time Step (CCPG) as a primary performance metric as it takes into account the cost of interprocess communication [64]. When run on a single core, 100% of the program runtime is spent on computation. As the number of processor cores increases, a larger portion of the runtime is spent on communication and therefore the cpu time taken to compute a single

grid-point increases. The amount of consumed compute resources T_p for a given simulation can be calculated given the wallclock runtime t and the number of processors used p, as shown in Equation 4.3.

$$T_p = t \cdot p \tag{4.3}$$

To provide a meaningful comparison between core counts, the CCPG must be calculated. Given the number of timesteps N_t and number of grid points N_g, we can calculate the total simulation CCPG, C_{tg} as shown in Equation 4.4.

$$C_{tg} = \frac{T_p}{N_t \cdot N_g} \tag{4.4}$$

Although increasing MIMD parallelism by introducing additional processor cores decreases the overall runtime, a greater portion of the runtime is spend idle waiting for data to be sent between processors. The C_{tg} metric doesn't discriminate based on wallclock runtime, and provides a solid basis for comparison between model resolutions and number of processor cores.

Operational intensity

The operational intensity I of a code or compute kernel is defined as the ratio of work W to the memory traffic Q [65]. It is a commonly used metric to assist in the identification of performance bottlenecks of high-performance codes, especially when used together with a roofline model [65]. Operational intensity is formally defined in Equation 4.5.

$$I = \frac{W}{Q} \tag{4.5}$$

For the analysis performed in this research project, W denotes the number of FLOPS, and Q denotes the total amount of memory transferred in Bytes. This results in operational intensity measured in FLOPS/Byte.

Summary

To ensure simplicity, the wallclock runtime is the primary performance metric used throughout this report. However, it is important to consider other metrics as they can uncover important features of the code that are overlooked by runtime alone. Values for all four metrics defined in this section have been calculated using the data collected as part of this research project.

The benchmarks presented in this chapter provide a comparison of the different hardware limitations of each of the processors used in this project. Although synthetic benchmarks give an indication as to the raw performance of the processors, they are unable to predict the performance of more complex codes like Isca.

CHAPTER 5

Porting

In the context of software development, porting refers to the process of modifying an existing codebase in order for it to run on a different system than it was originally written for. This chapter gives an overview of some of the tools and techniques used when porting Isca, and presents some of the challenges encountered in doing so. Many small changes have been made to the codebase to enable the model to compile and run using a selection of commonly-used compilers, some of which can be found in appendix A.

5.1 Compilers and MPI libraries

Different compilers produce different instructions for the same code. To allow for the best comparison between processors, Isca was compiled using a number of different compilers and MPI libraries to find the compiler that produces the fasted running executable for the given hardware. Table 5.1 shows the different configurations used to compile Isca on each of the clusters used in this study.

Table 5.1: Compilers and MPI libraries used for benchmarking.

Cluster	Processor Family	Fortran Compiler	MPI library
BCP3	Sandy Bridge	GNU 7.1.0	OpenMPI
		Intel 13.0.1	OpenMPI
BCP4	Broadwell	GNU 7.2.0	OpenMPI
		Intel 18.0.3	Intel MPI
BP	Skylake	Intel 19.0.3	Intel MPI
Isambard	ThunderX2	CCE 8.7.9	Cray MPI
		GNU 8.2.0	Cray MPI

Isca uses a Perl script called MakeMakeFile (MKMF) to construct makefiles for different model configurations. Before compilation, Isca runs a series of 'template scripts' to export environment variables and to load relevant module files to be used by MKMF. In order to compile on a new system, a new template script must be written to setup the compilation environment for the machine in question. Although Isca provides some example scripts to do this on existing systems, a new script had to be written for each compiler and processor pair in this study. Two examples of such scripts can be found in Appendix C.

5.1.1 GNU Compiler Collection

The GNU Compiler Collection (GCC) is a selection of compilers for various programming languages and is produced and maintained by the GNU project. GCC is available on many different computer architectures, providing the same interfaces and compiler flags on each. This makes it a

convenient compiler for porting code, as similar configurations can be used on different machines. The Isca codebase already has an existing GCC template script, however it required some minor changes to allow for compilation on each system. This involved selecting the correct module files to be loaded when the script was run, and exporting relevant compiler and linking flags.

5.1.2   Intel Compiler Collection

The Intel Compiler Collection (ICC) provides numerous premium compilers specifically for Intel-based machines, and is bundled as part of Intel Parallel Studio XE. As Intel develops its compilers alongside its hardware, ICC generally produces well-optimised instructions, however they are not portable and are limited to Intel processors only. Contained within ICC is the Intel MPI library, which is focussed on making parallel applications perform better on Intel-based clusters.

The existing Intel template script provided by Isca required few modification to compile the model on each system, however the locations of some libraries needed to be specified. Additionally, the NetCDF library needed to be recompiled using the latest version of the Intel compiler in order to work.

5.1.3   Cray Compiling Environment

The Cray Compiling Environment (CCE) is a Fortran 90 compiler developed by Cray Inc. This compiler is relatively new in comparison to the Intel and GNU compilers, and as such is strict to the Fortran standard. This caused many issues when porting the code using this compiler, and flagged up a number of issues with the Isca codebase. The process of porting for CCE turned into a stringent debugging exercise that has inevitably improved the reproducibility of the code on different platforms. The following subsections describe some of the code changes required to compile and run Isca using the CCE compiler.

Implicit type conversion

To provide interprocess communication, Isca uses a *'Massively-parallel'* module, named MPP. It is a set of simple calls to provide a uniform interface to a collection of commonly used message-passing routines for climate modelling, implemented in different libraries [15]. This module defines many subroutines that depend on the definition of the `MPP_DEFAULT_VALUE_` macro, which is defined using preprocessor directives at compile time. The `MPP_DEFAULT_VALUE_` can be assigned as either real, integer or logical. As an extension for backwards compatibility with other compilers, the GNU and Intel compilers allow for the implicit conversion of logicals to numericals and vice versa. When converting from a logical to an integer, the numeric value of `.false.` is 0, and that of `.true.` is 1. When converting from integer to logical, the value 0 is interpreted as `.false.` and any non-zero value is interpreted as `.true.`. This does not conform to the Fortran 90 standard, which disallows implicit conversion between numeric variables and logicals [66, 67]. This error was found throughout the codebase and changes were made to resolve this issue by creating a new macro `MPP_DEFAULT_TYPE_`, which is used to define the type of variables assigned using the `MPP_DEFAULT_VALUE_` macro.

Namelist read errors

Isca uses Fortran namelist files to read parameters into existing variables and data structures at runtime. Using CCE, many of the namelist files were being read incorrectly as Isca did not

open and close files between separate reads, which caused the code to hang during execution. Additionally, the Cray compiler requires that the representation of the value in the namelist file reflects the type of variable that it will be used for. This means that an integer value must be stored in the namelist as `variable = 1`, and not `variable = 1.0`.

Ambiguous arithmetic

The Cray compiler uses a different order of precedence for operations, and required brackets around some arithmetic where it could be considered ambiguous. This was found in few places in the codebase, and was trivial to fix once identified.

5.1.4 Discussion

As the Fortran standard has evolved over the past twenty years, many features that were once commonplace are no longer deemed to fit the language standard, and are not supported by newer compilers. Some of the more popular compilers like GCC and ICC have been updated to allow for backwards compatibility with legacy code, however this is not the case for the CCE compiler, which strictly follows the Fortran standard.

Both ICC and GCC overlook many negligent programming practices. However to remain portable, codes should be written to the standards of the programming language. Many legacy codes suffer from this issue whereby outdated code remains unchanged throughout many years of use, and part of this research project was to update Isca to improve its portability.

5.2 Cluster feedback

5.2.1 Stack size

Prior to this project, the default stack size set by the PBS job scheduler on BP was 8 KB. However, as Isca uses a large amount of memory this caused a stack overflow error when running the model at resolutions greater than T42. Due to some configuration restraints on the cluster, the PBS scheduler does not allow for the stack size to be increased using `ulimit -s unlimited`, as used in Isca's run script. To resolve this issue the default stack size was increased to 64 MB by the system administrator.

As a temporary work around before this issue was resolved, and before interactive jobs were available on the cluster, a regular job can be submitted to the queue that sleeps for an hour in the submission script. The details of the job can be found using the `qstat -f <jobid>` PBS command, which can then be used to SSH to the node running the sleeping job. As PBS has not been used to access to the node, the stack size can be increased using the command `ulimit -s unlimited`, and the code will then run as if in an interactive job. Most of the single-node runtimes for BluePebble were collected using this technique as modifying the cluster configuration was not immediately possible.

5.2.2 Strict processor enforcement

Isca's Python library is multithreaded, creating additional threads of execution when running experiments. This caused some issues when the model was run on BluePebble as its job scheduler was configured to strictly enforce the CPU limitations defined in the job submission script. After

running for an arbitrary amount of time the job would fail as additional Python threads were created, causing the CPU to try to burst past the scheduler limit. This issue took many weeks to fix and required working alongside the BluePebble system administrator.

5.3 Libraries and dependencies

Although many of the libraries required by Isca were already available as module files, in some cases they were not. This meant that they needed to be built in the $HOME directory to allow for the model to be compiled. These builds were then used to create module files by the system administrators of the relevant cluster. Throughout the course of the project, the NetCDF, Git, FFTW, Anaconda Python, zlib and HDF5 software packages were installed multiple times using different compilers.

5.4 Development tools

All code developments were made remotely over SSH and all work was done on the filesystem of each supercomputer. Microsoft Visual Studio Code has a Remote-SSH plugin that allows for files to be edited as if they were on a local machine. This plugin is still in its beta phase of development, and can therefore be unreliable. When it failed, work continued using both the emacs and vim text editors depending on the tools available on the cluster. To allow for code changes to be synchronised across machines, a new fork of the Isca Git repository was created. Each cluster had their own development branch as well as a main development branch for merging changes between them.

5.5 Verification of results

When porting a codebase it is important to test that the changes made to the code are backward compatible. This means that all changes must be non-intrusive and configurations must default to the original behaviour. In the case of Isca, all code changes that have been made to run the model on a different cluster have been tested on the BCP4 supercomputer to ensure that they produce the same outputs.

5.5.1 Units of last place

To ensure that the model produces the same results on each system, the model outputs have been checked using the Units of Last Place (ULP) numerical analysis technique, which can be used to measure the spacing between floating point numbers. As the whole real line cannot be represented in memory, there is a minimum difference between two numbers occupying the full space offered by floating point numbers [68]. NetCDF files aim to record data in a continuous fashion, which is an impossible task for the discrete numbers used in computational simulations like Isca [38].

The outputs of a simulation run by Isca can be verified by comparing the ULP of each parameter in the resulting NetCDF file. As the model is chaotic, even small changes to model parameters can produce vastly different results. However, as the model is not stochastic, the same simulation configuration ran on two separate machines should produce identical results, assuming that the machines store variables to the same degree of precision.

Rounding errors

Rounding errors are a commonly occurring quantisation problem in scientific codes [68]. Although double-precision floating point variables can store numbers to a high degree of precision, they can only store a finite number of digits. Rounding errors are a result of performing arithmetic on continuous numbers in a discrete representation. The IEEE Standard for Floating-Point Arithmetic (IEEE 754) states that all floating point arithmetic must be correctly rounded to within 0.5 ULP of the true mathematical result, therefore any differences greater that 1 ULP suggest inconsistencies in the code [68, 69].

5.5.2 Program verification

A C++ program was written by Gethin Williams in 2009, and modified for this research project to measure the difference in ULP between NetCDF files obtained on different machines [70]. The program allows for a tolerance to be given to accommodate any rounding errors that may have accumulated throughout the course of the simulation. Due to the differences in compiler and processor architecture a tolerance of 2 ULP was deemed acceptable. All changes to the Isca codebase were verified using this metric.

5.6 Summary

todo

Part II

Benchmarking, performance analysis and optimisation

CHAPTER **6**

Experimental Methodology

This chapter outlines the experimental methodology used for benchmarking and analysing the performance of Isca.

6.1 Model configurations

Isca is a coupled model, allowing for the simulation of either the atmospheric or oceanic components of a planet, or both components simultaneously. The complexity of these simulations are defined at compile time and allow for different algorithms to be applied depending on the model configuration. Although this means that the model is highly flexible, it introduces a challenge when trying to profile the code as a whole, as optimising one configuration may have no impact on another. This research project focuses on the optimisation of two test configurations: the well-known Held-Suarez configuration and a Grey-Mars radiation model.

6.1.1 Held-Suarez test case

The Held-Suarez simulation was designed by Held and Suarez in 1994 to allow for comparison between GCMs [71]. It is well studied and is considered to be a gold standard for benchmarking climate models [72, 73, 74]. It is configured to simulate only the 'dynamical core' of a planet, which contains the discretised equations of motion and state. In terms of complexity, the Held-Suarez model is one of the simplest configurations available to Isca and is essentially the foundations upon which more complex models are built. The simulation maintains a constant climate throughout its duration by forcing many parameters to predefined values. This allows for the dynamical core to be run by itself without the need for coupling with other complex model components. This makes the Held-Suarez configuration a good candidate for benchmarking and optimisation as the dynamical core code is used in all other model configurations that model the atmosphere.

Isca's Held-Suarez simulation computes over an idealised model of the Earth. In terms of measuring its performance, the simulation has been run for 12 model months with each month simplified to last 30 days, for a total of 360 model days per simulation. This length of time was chosen to allow for the performance to be measured at each phase of the Earth's orbit of the Sun. The Held-Suarez simulation does not use solar radiation as a model parameter, however it is important to measure the performance for a full year to model other seasonal parameters.

6.1.2 Grey-Mars test case

The Grey-Mars simulation is configured to simulate the effect of grey radiation on the planet Mars over time, building upon the dynamical core code used in the Held-Suarez configuration. It was chosen for optimisation due to its frequent use by academics at the University of Bristol, as well as to demonstrate of some of the more complex features of Isca.

The axes of both Earth and Mars are not orthogonal to their orbit of the sun; Earth's axis is at a 23.5° tilt and Mars' axis is at 25° [75]. These tilted axes are responsible for the seasons, however this causes many climate models to suffer from a load-balancing issue whereby calculations take longer on the side of the planet facing the sun due to increased levels of thermal radiation [76]. To test for this, the Grey-Mars configuration has been run for 690 model days to account for the 687 martian days it takes for Mars to orbit the Sun [77]. This simulation is broken into 23 sub-simulations each lasting 30 days.

6.1.3 Domain decomposition

When running in parallel Isca requires that the number of latitudes divided by the number of cores must be divisible by 2 [11]. Therefore the T21 resolution, which splits the planetary domain into 32 latitudes, can be run on 1, 2, 4, 8 or 16 cores. The simulation cannot be run on more processor cores as the number of processors will be equal to the number of latitude bands. A full list of compatible resolutions and core counts can be found in Table 6.1.

Table 6.1: Resolutions and their compatible core counts. Lower resolutions are limited in the number of cores they can use.

Truncation	Latitudes×longitudes	Available core count
T21	32×64	{1, 2, 4, 8, 16}
T42	64×128	{1, 2, 4, 8, 16, 32}
T85	128×256	{1, 2, 4, 8, 16, 32, 64}
T170	256×512	{1, 2, 4, 8, 16, 32, 64, 128}

This inherent domain decomposition constraint imposed by the model means that some nodes are unable to run Isca at full capacity. For example, a single node configuration of BCP4 can only run Isca at a maximum of 16 out of 28 cores per node. This poses an interesting problem, whereby the model is a better fit for some nodes than others simply due of the number of processor cores per node.

Although Isca can vary both in its spatial and temporal resolution, the scaling study undertaken as part of this research project focuses solely on variations in spatial resolution. This decision was made in order to simplify the process of performance analysis by limiting the number of problem sizes. Additionally, changes to performance as a result of time stepping are generally predictable, and will not contribute to a further understanding of the code. A model that performs twice as many time steps will perform twice as many calculations and will therefore be twice as slow.

6.2 Automated data collection

In order to collect reliable and consistent data it is important to use the same method of data collection for different configurations. When benchmarking high performance applications data collection can be a laborious process. The runtimes of the configurations used in this study are in the range of 3 minutes for simple configurations at low resolutions up to 10 days for high resolution complex scenarios running in serial. Running this range of simulations manually would be incredibly time consuming, therefore a Python library was written to automate this process. The source code for this library can be found on GitHub [78].

The Python library was written to sequentially run a number of different experimental configurations given a set of parameters, including the core count, resolution and model configuration.

This allowed for a number of experiments to be run from within a single job submission script with the results of each experiment automatically stored in a spreadsheet. Each experiment defined by the Python script recorded the total time taken to complete the simulation as well as each thirty-day epoch.

In order to collect reliable data a full node was used for each experiment. Even when run in serial, the model used the resources of an entire node so that the performance would not be affected by shared resource usage by other programs running on the cluster. To account for variations in runtime caused by factors outside the control of the experiment, all runtimes reported in this chapter are the mean value of three repeat measurements, unless stated otherwise. The results presented in the following section are the consequence of over 1,000 hours of experimental runtime.

6.2.1 Job submission

BCP3 uses the PBS job scheduler, BP and Isambard use the PBS Pro job scheduler and BCP4 uses the SLURM scheduler. These are tools that allow for applications to be submitted to a queue and run on a compute node when the required resources are available. Each of these schedulers use a slightly different syntax, therefore a number of submission scripts have been created for each cluster based on the amount of resources required and expected runtime. Example job submission scripts can be found in Appendix D.

As the clusters used in this project are actively used for research, there is naturally some competition for compute resources between users. A trial and error approach was used to find the right parameters for the job script in order for the job to be processed from the queue quickly, whilst ensuring that the runtime was adequate to complete the entirety of the job.

6.3 Experiments

The collective aim of the following experiments was to characterise the code, to identify potential optimisations and to provide a comparison of the processors themselves.

6.3.1 Experiment A: Scaling study

To determine how well the model performs when presented with additional compute resources, Isca was run on 1 core up to and including the maximum number of cores available on a node of each cluster. Additionally, it was run across all possible combinations of model configuration and resolution in order to measure its performance at various levels of complexity and realism. To allow for comparison between processors, the results have been reported as both wallclock runtime and speedup relative to the serial performance.

6.3.2 Experiment B: Compiler comparison

To find the optimal compilation settings for each processor, both the Held-Suarez and Grey-Mars model configurations were complied using two different compilers on each cluster, excluding BluePebble. All cases compiled using the GNU compiler used the same flags, and all cases compiled using the Intel compiler used the same flags. The flags used for the GNU compiler on Isambard were those recommended by the ARM64 Best Practices Guide, and the equivalent flags were used on the Intel machines [79]. At the time of writing, only the Intel compiler and MPI

library were available on BluePebble, therefore there is no comparison of different compilers on a Skylake node.

Table 6.2: Number of processor cores used to measure the performance of different compilers at the T21 and T42 resolutions.

Processor Family	Number of cores	
	T21	T42
Sandy Bridge	16	16
Broadwell	16	16
ThunderX2	16	32

For this test, the per-node performance was considered only. The model was run on up to the maximum number of cores available on each node for the given model configuration (Table 6.2). This provided a comparison of the compilers in relation to the performance available on other processors. The observations made in this experiment informed the choice of compiler for all other experiments, which used ICC for all Intel nodes and GCC for the ThunderX2.

6.3.3   Experiment C: Vectorisation analysis

To determine the importance of instruction-level parallelism, the per-node performance of the code was measured with SIMD instructions enabled and disabled for the Held-Suarez and Grey-Mars model configurations running at T42 resolution. Isca was compiled using the relevant flags to disable vectorisation, and vector reports were produced to ensure that no automatic vectorisation occurred. For this experiment, all other optimisations were enabled.

6.3.4   Experiment D: Computation rate

The CCPG metric defined in Section 4.2 was calculated to determine how the cost to compute a single grid point changes as the model uses more compute resources. It can be expected that the computational cost increases as more compute resources are utilised as more time will be spent on communication between processors ranks.

6.3.5   Experiment E: Communication analysis

This experiment measured the percentage of runtime spent in the MPI library and the total communication time between processors. This was done to find the percentage of total runtime spent in communication, and to determine the degree to which load imbalance affects the performance of the model. To see if the workload is equal for all processors at each epoch of the simulation, the communication times were compared for the first and thirteenth epochs of the Grey-Mars model configuration (Figure 6.1).

6.3.6   Experiment F: Runtime variation

Isca simulations are made up of many sub-simulations called epochs, with each epoch often lasting for one model month at a time. Epochs differ from time steps, which describe the amount of time between each global calculation. To determine if any parts of the simulation are more
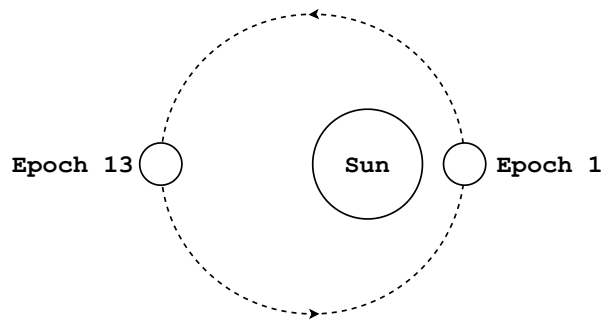
Fig. 6.1: Position of the planet Mars at epoch 1 and epoch 13.

computationally demanding than others, the runtime of each epoch was measured for both the Held-Suarez and Grey-Mars configurations at various model resolutions.

6.3.7 Experiment G: Roofline analysis

A roofline model is an insightful visual performance analysis technique used to identify the hardware-limiting factors of an application, or compute kernels within an application. It plots the floating point performance as a function of peak machine performance, peak machine memory-bandwidth and the operational intensity of the code itself [65]. The performance limiting factor of a code or compute kernel can be determined by looking at where it sits on the roofline. Points underneath the memory bandwidth ceiling indicate that the code is bound by memory bandwidth, whereas a point directly underneath the peak performance ceiling suggests that the code is bound by the available computational resources.

6.4 Summary

todo

CHAPTER 7

Results

This chapter presents the findings of the experiments described in Section 6.3, demonstrating an extensive performance analysis of Isca running two unique model configurations on four different compute nodes. These results have been used to inform the design and implementation of two performance optimisations in Chapter 8.

7.1 Experiment A: Scaling study

In the following section, the vertical coloured bars on the y plane indicate the maximum number of processors available on each cluster.

7.1.1 Results
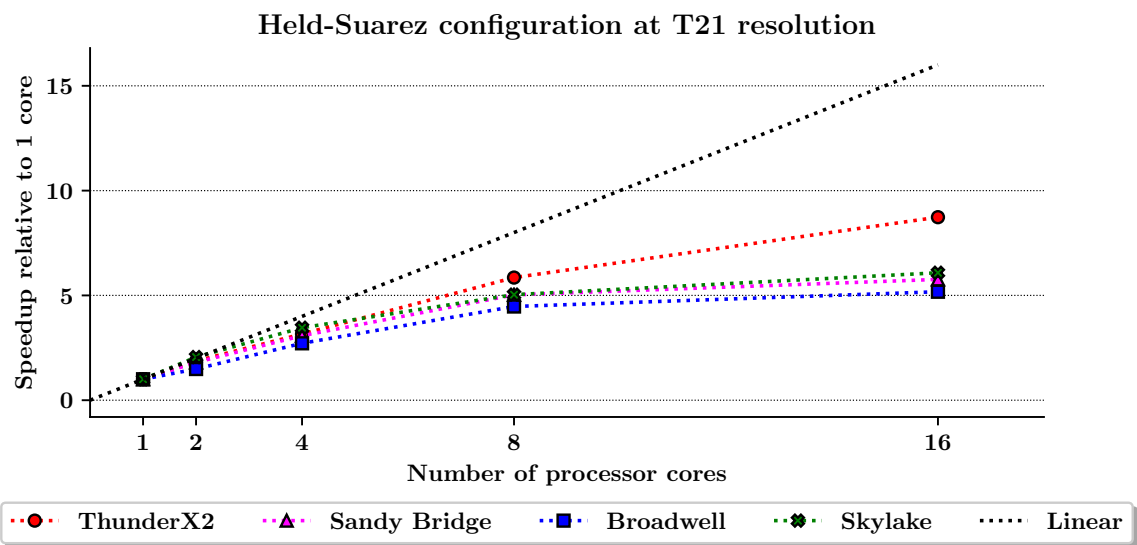
Fig. 7.1: Parallel speedup relative to serial performance for the Held-Suarez configuration running at T21 resolution.

When Isca is run on 8 cores the Sandy Bridge, Broadwell and Skylake processors see a performance improvement of 5.1×, 4.5× and 5.0× relative to the serial runtime, respectively, before plateauing between 8 and 16 processor cores (Figure 7.1). The ThunderX2 speeds up by 5.9× when run on 8 cores, and 8.7× when run on 16 cores. When increasing the number of processor cores from 8 to 16 for the Held-Suarez configuration, there is only an approximate 1.15× performance gain for the Intel processors. This is typical of many parallel codes, whereby the performance benefit of additional compute resources decreases as more processor cores are utilised [7]. As this problem size is small, more time is spent in communication relative to compute when a greater number of processor cores are used.
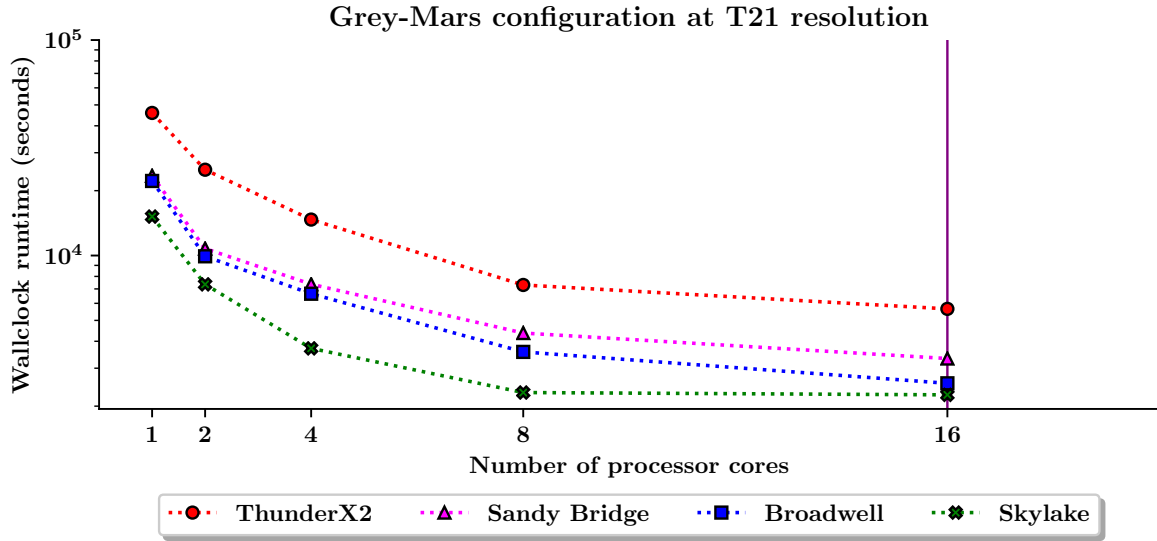
Fig. 7.2: Wallclock runtime of the Grey-Mars configuration running at T21 resolution across all processor architectures.

The scaling curve in Figure 7.2 shows a sublinear plateau for all node configurations, whereby the wallclock runtime of all four processors reduces steadily from 1 to 8 processor cores. The wallclock runtime is greatest when the program is run in serial and lowest when run on 16 cores, which is the maximum number of cores possible for this resolution. The trend observed for the Grey-Mars configuration (Figure 7.2) is comparable to that of the Held-Suarez result (Figure 7.1), whereby the slowest runtime is the serial case and the fastest is the 16 core case. The Skylake processor massively outperforms all other processors when run on 8 cores, however the performance gains become quickly saturated when run on 16 cores, running just 1.02× faster than the 8 core case.

Fig. 7.3: Wallclock runtime of the Held-Suarez configuration running at T42 resolution across all processor architectures.

Fig. 7.4: Speedup of the Held-Suarez configuration running at T42 resolution relative to serial runtime across all processor architectures.

Increasing the spatial resolution to T42 (Figures 7.3, 7.4) presents a similar scaling curve to that observed for the T21 resolution (Figure 7.2). For all processors except Sandy Bridge, the slowest runtime is measured for the serial code and the performance improves until the program is run on 16 cores. For the Intel processors, running on more than 16 cores requires multiple nodes, which has a dramatic impact on the performance of the Sandy Bridge and Skylake processors. At 32 cores the performance of the Sandy Bridge and Skylake processors reduces from 9.2× to 0.1× and 12.0× to 3.0×, respectively. The Broadwell and ThunderX2 processors improve at this core count, from 8.2× to 10.2× and 12.7× to 18.7×, respectively. Although the ThunderX2 does not provide the fastest overall runtime (Figure 7.3), plotting the speedup relative to the serial runtime demonstrates that it exhibits the best level of scaling (Figure 7.4). This can be attributed to the large core count of the processor, which means that it does not have to rely on internode communication.
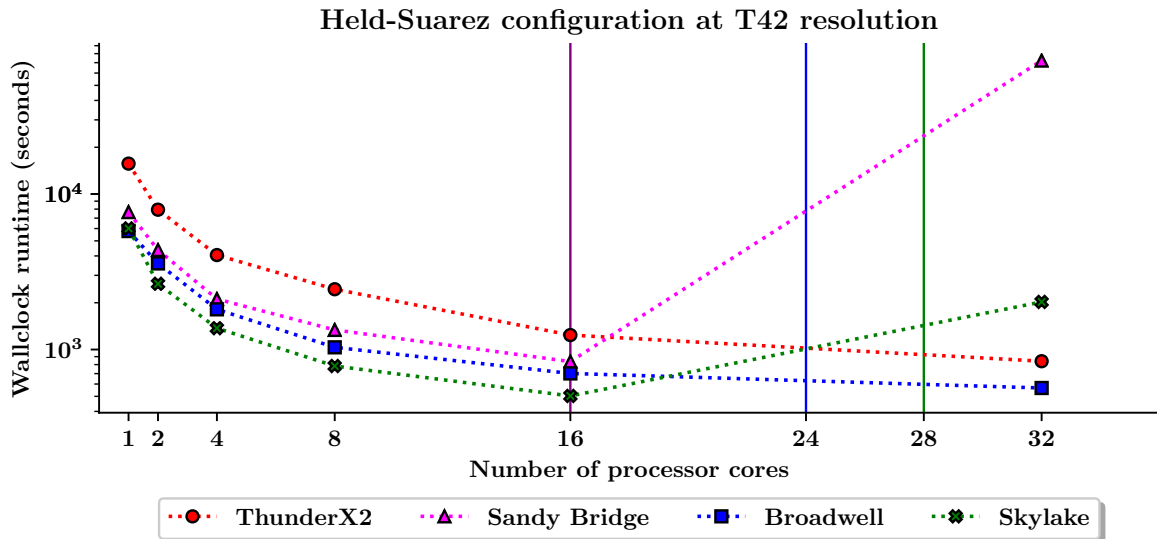
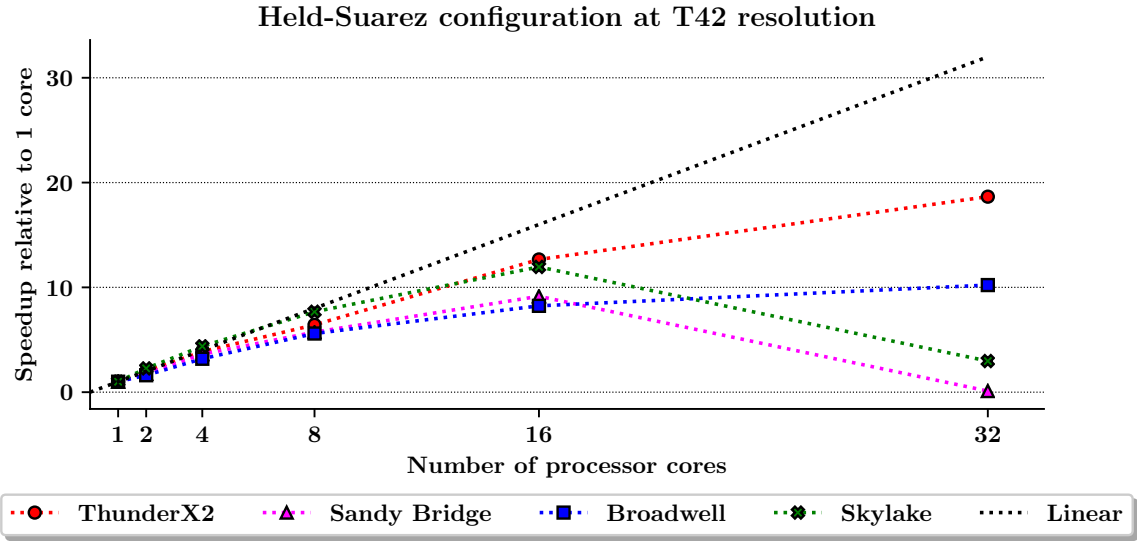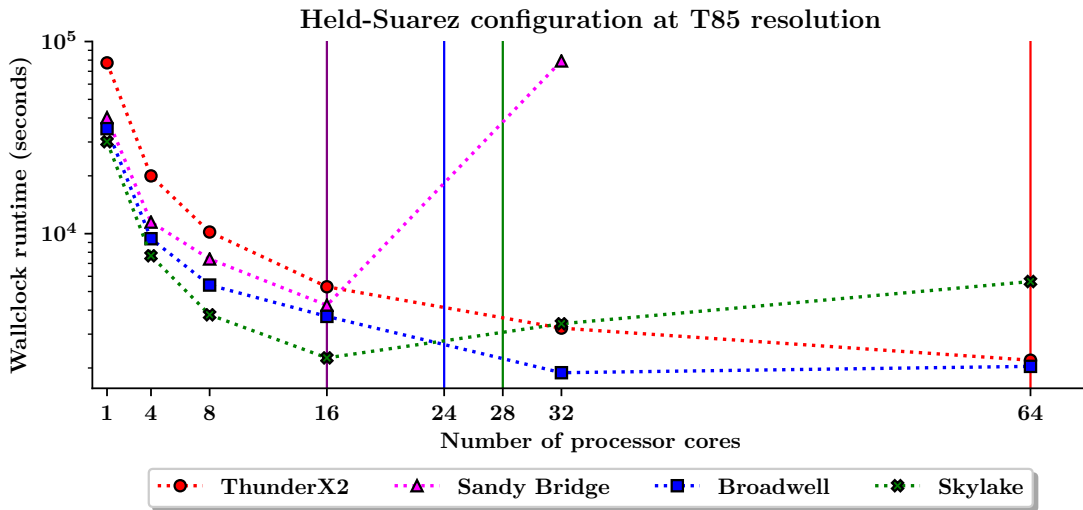Fig. 7.5: Wallclock runtime of the Held-Suarez configuration running at T85 resolution across all processor architectures.
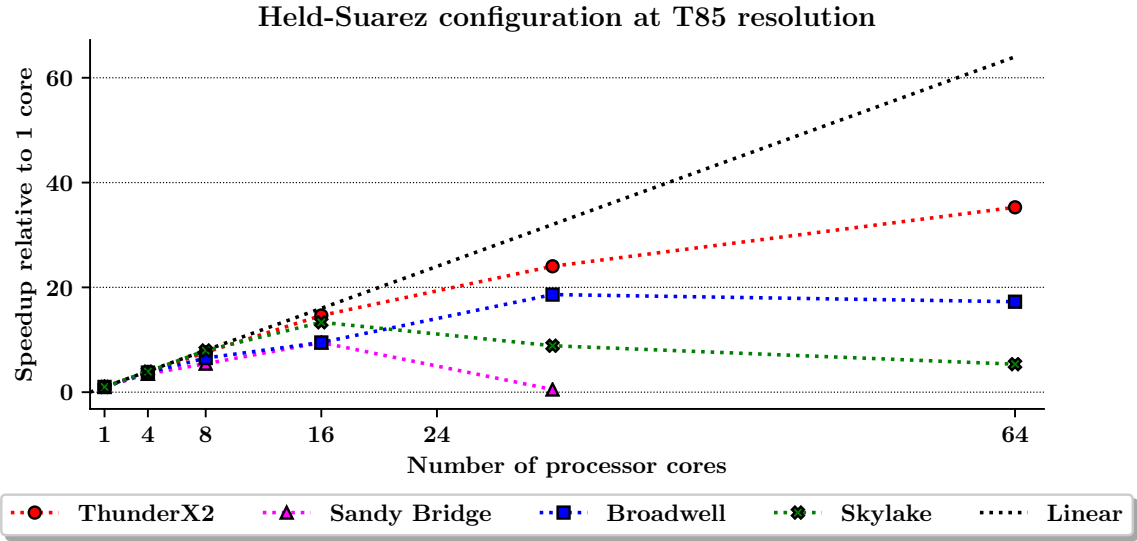
Fig. 7.6: Speedup of the Held-Suarez configuration running at T85 resolution relative to serial runtime across all processor architectures.

For the T85 resolution (Figures 7.5 and 7.6), the performance of the Broadwell processor begins to decline when run on 64 cores across three nodes, reducing from a $18.6\times$ speedup at 32 cores to a $17.3\times$ speedup at 64 cores (Figures and 7.5). This suggests that this is the point at which the cost of communication outweighs the benefit of additional parallelism for this processor. The performance of the ThunderX2 continues to improve when run on 64 cores, increasing from $24.0\times$ at 32 cores to $35.3\times$ at 64 cores.

7.1.2 Conclusions and discussion

This scaling study highlighted some of the architectural differences between Intel and Arm processors. Arm's approach to processor design relies on a greater number of simple processor cores, in comparison to Intel's fewer, more complex cores. This design complemented the Isca code by keeping communication inside a single node for resolutions of T85 and below, allowing for a higher degree of scalability to that of the Intel processors.

MPI is primarily used for communication between nodes, however messages are exchanged using shared memory when used within a single node [37]. This can greatly reduce the amount of time spent on communication as there is no data transfer between nodes, which can be an expensive process. This is likely what is causing Isca to scale well on the ThunderX2. In contrast, memory-bandwidth bound codes can see significant gains to performance when run on multiple nodes, which increases the total memory bandwidth and therefore reduces the cache-contention between processors [80].

The performance of the Intel processors suffered when run on multiple nodes. This is to be expected on the Skylake nodes as the BP supercomputer does not have a high-speed interconnect, using only ethernet to connect compute nodes. Interestingly, the lowest performance observed for the dual-node configuration is the Sandy Bridge processor, which takes $82\times$ longer to complete the same job than when running on a single node. BCP3 uses QDR InfiniBand, which has a theoretical throughput of 8 GB/s per connection and should therefore not exhibit this behaviour [81]. The Sandy Bridge node was the only Intel configuration to use OpenMPI instead of Intel MPI. Unlike Intel MPI, OpenMPI has not been developed specifically for Intel compute nodes,

and this could have affected the internode performance for this configuration. However, it is unlikely that this is the sole reason for the poor internode performance. Both the ThunderX2 and Broadwell processors do not exhibit this behaviour when run on 32 and 64 cores, which suggests that the issue is most likely caused by internode communication rather than a bug in the model that manifests at higher core counts.

Due to restrictions imposed by domain decomposition, the Grey-Mars configuration cannot be run at resolutions higher than T42. Because of this, the results for the T85 resolution are limited to the Held-Suarez configuration only. Additionally, the time limit imposed by the queuing system prevented results from being gathered for the Sandy Bridge processor when running on 64 cores as the runtime was greater than 360 hours, which is the longest amount of time available for a single job on the BCP3 supercomputer.

7.2 Experiment B: Compiler comparison

This experiment measured the wallclock runtime of Isca when complied using the ICC, GCC and CCE compilers using two different model configurations and resolutions (Tables 5.1 and 6.2).

7.2.1 Results

For all configurations tested on Intel nodes ICC outperformed GCC (Figure 7.7). ICC provides a mean performance improvement of 1.26× over GCC across both the T21 and T42 resolutions. On the ThunderX2, GCC was 1.4× faster than CCE at the T21 resolution but just 1.01× faster at the T42 resolution.
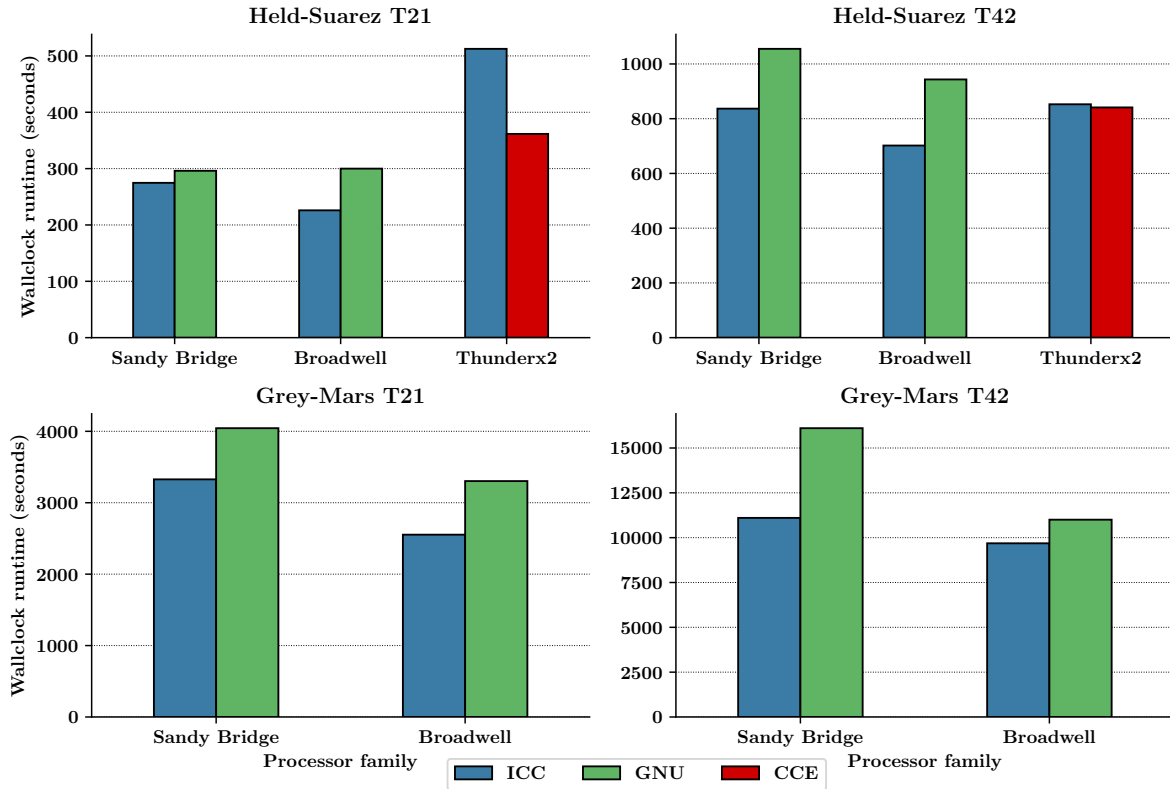
Fig. 7.7: Runtimes for the Held-Suarez and Grey-Mars configurations using different compilers.

7.2.2 Conclusions and discussion

It can be expected that ICC outperforms GCC on Intel hardware as Intel develops their compilers alongside their processors. Consequently, the Intel compilers produce well-optimised instructions for the architecture. This experiment confirmed this expectation as ICC surpassed GCC in all cases. For the ThunderX2, GCC outperformed CCE. For both compilers, flags were specified to produce hardware specific instructions for the ThunderX2 processor, however neither compiler has been exclusively developed for the Armv8 architecture. Therefore, this performance difference could be explained by the the maturity of GCC in comparison to CCE as the compiler has been in constant development since 1987, however there is no evidence to support this claim.

7.3 Experiment C: Vectorisation analysis

This experiment measured the performance speedup of Isca when the model was compiled to use SIMD instructions, compared to when run in scalar.

7.3.1 Results

Fig. 7.8: Speedup of the vectorised code relative to scalar at T42 resolution.

Only marginal performance gains are observed when running Isca using SIMD instructions compared to scalar (Figure 7.8). For the Held-Suarez model there is a $1.07\times$, $1.25\times$, $1.13\times$ and $1.01\times$ performance improvement for the Sandy Bridge, Broadwell, Skylake and ThunderX2 processors, respectively. For the Grey-Mars configuration there is a $1.07\times$, $1.02\times$, $1.11\times$ and $1.06\times$ performance improvement for the same processors.

7.3.2 Conclusions and discussion

Some of the most time-consuming compute kernels in Isca operate over arrays of double-precision complex numbers. In the Fortran programming language a complex number is composed of a pair of floating point numbers, representing both real and imaginary parts of the complex number. This means that a double-precision complex number of kind 8 uses 128 bits of memory; both real and imaginary parts of the number are a real value of 8 bytes each. This means that vectorisation is costly in parts of the code that iterate over complex data structures, and impossible on the 128-bit registers used in Intels SSE, and Arms NEON SIMD extensions. Interestingly, Intel's cost

model often determines that there is no benefit to using SIMD instructions on arrays of double-precision complex numbers, even on the 256-bit and 512-bit registers available through AVX-2 and AVX-512, respectively.

Small but consistent performance gains were measured when the model was compiled to use SIMD instructions. This suggests that the model is not heavily exploiting vectorisation to provide performance. To improve performance, For the Held-Suarez configuration the ThunderX2 saw the least improvement, which was expected as the ThunderX2 only has 128-bit vector registers. Following the ThunderX2 was the Sandy Bridge processor, which uses the AVX instruction set. Although this allows for a vector width of up to 256-bits it does not include fused multiply-accumulate operations like the AVX-2 instructions used by Broadwell and the AVX-512 instructions used by Skylake, and this is reflected by its performance [82, 83].

7.4 Experiment D: Computation rate

This experiment measured the cost of computation relative to the number of concurrently utilised processors using the CCPG metric defined in Section 4.2.
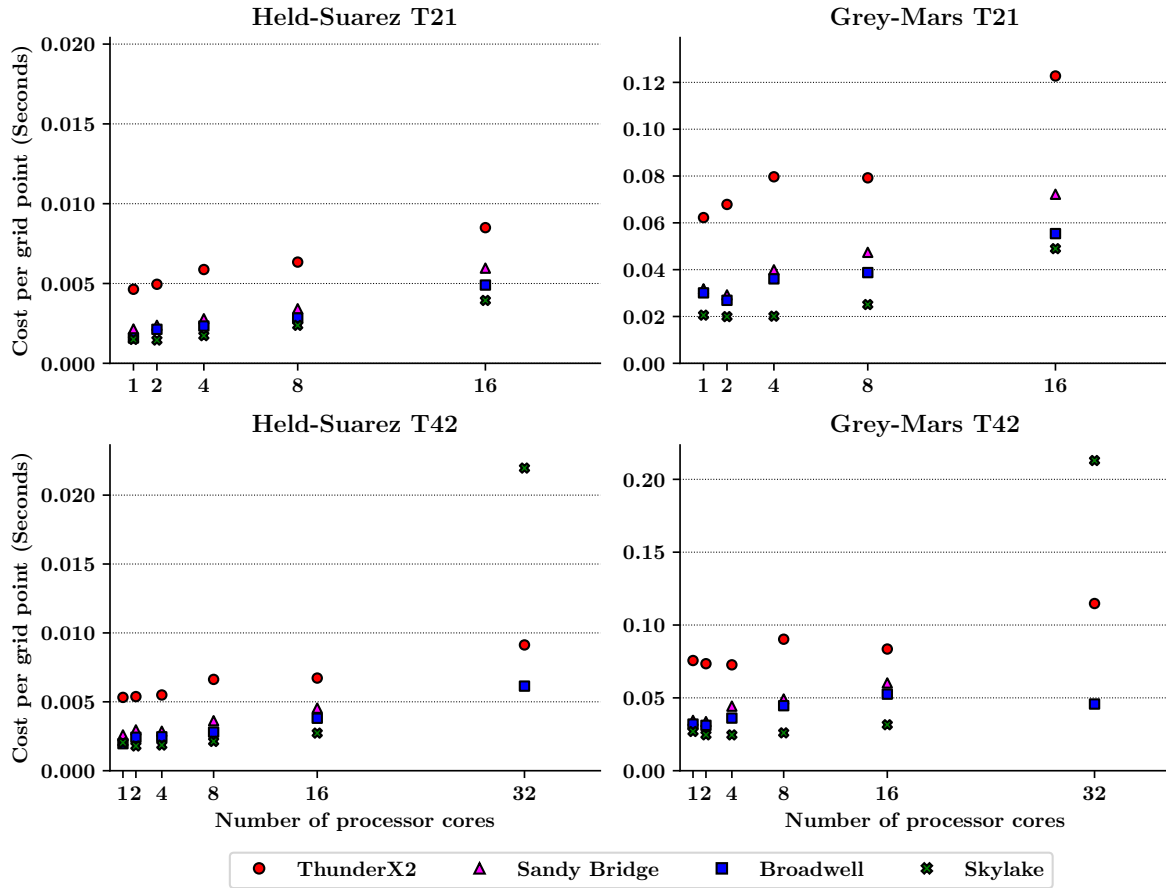
7.4.1 Results

Fig. 7.9: Cost per grid point for the Held-Suarez and Grey-Mars configurations at T21 and T42 resolutions.

For the Held-Suarez configuration running at the T21 resolution the introduction of parallelism

causes an increase in CCPG for all node configurations except Skylake (Figure 7.9). The CCPG decreased for the Skylake node when parallelism was introduced to the model. Increasing the amount of parallelism past the utilisation of two cores causes the CCPG to increase almost linearly for all processors at this resolution. The same trend was observed for the Held-Suarez configuration when running at the T42 resolution. However, for the dual-node case the CCPG sharply increases for the Skylake node with a cost 6.7× greater than when run on the maximum capacity of a single node.

For Intel nodes running the Grey-Mars configuration at the T21 resolution, the CCPG initially decreases when parallelism is introduced. However, running on more than 4 processor cores increases the CCPG. This is not the case for the ThunderX2, for which the CCPG increases until it is run on 8 processor cores at which a plateau is reached, before increasing again at 32 cores. This same pattern is observed for the Grey-Mars configuration running at the T42 resolution, however the CCPG dips for the ThunderX2 when run on 16 cores, rather than reaching a plateau.

7.4.2 Conclusions and discussion

Plotting the CCPG demonstrates that increasing the number of processors also increases the cost to compute a single grid point (Figure 7.9). Although there are more processors collectively working on the problem, a greater portion of the runtime is spent on communication and therefore processors spend more time idle. Although increasing the amount of parallelism causes the overall wallclock runtime to decrease, the total CPU time increases, which indicates that the code is less efficient as more processors are used for the same problem size.

The cost to compute a single grid cell increases from Skylake processor

7.5 Experiment E: Time spent in the MPI library

This experiment measured the percentage of runtime spent in the MPI library and the communication time between processors for a single epoch of an Isca experiment running at T42 resolution. The communication times were also measured for two different epochs of the Grey-Mars configuration.

7.5.1 Results

When running the Held-Suarez configuration on a Sandy Bridge node, each process spends between 40.8% and 48.1% of its total runtime in calls to MPI, and no discernible patterns can be identified through visual inspection of Figure 7.10. For the Grey-Mars configuration each process spends between 33.0% and 47.5% of its total runtime in calls to MPI. Processes 0-7 spend a much smaller percentage of their runtime in calls to MPI in comparison to processes 8-15, and process 0 spends a significantly smaller percentage of runtime in calls to MPI than any other process. Additionally, the time spent in the MPI library generally increases relative to the processor rank number.

The longest communication times are measured when processes 8-15 transmit data to process 0, with a mean communication time of 118.5 seconds (Figure 7.11). However, process 0 has the lowest sending times of any process, with a mean communication time of just 31.3 seconds. This suggests that process 0 is consistently taking the longest amount of time to reach points of synchronisation and can exchange data almost immediately upon reaching MPI barriers.
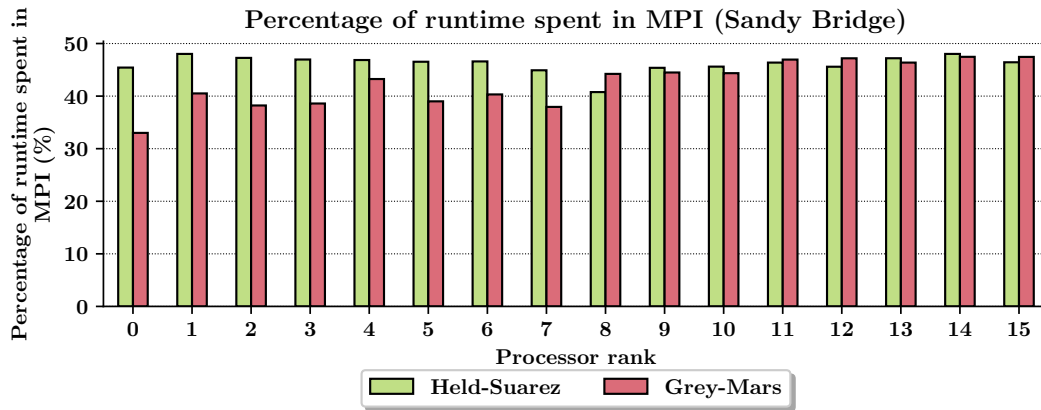
Fig. 7.10: Percentage of runtime spent in MPI across individual process ranks for both the Held-Suarez and Grey-Mars model configurations on a Sandy Bridge node.
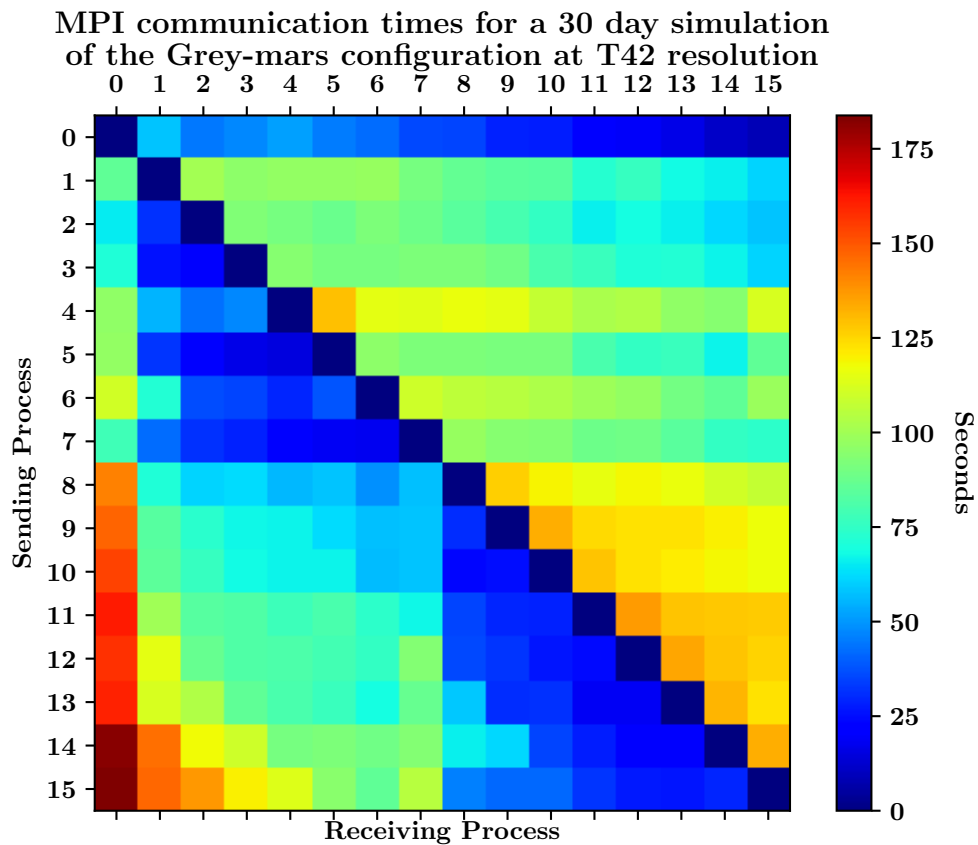

Fig. 7.11: Communication matrix for the Grey-Mars model configuration when run at the T42 resolution. Communication time has been measured as the sum of all time spent inside the MPI library.
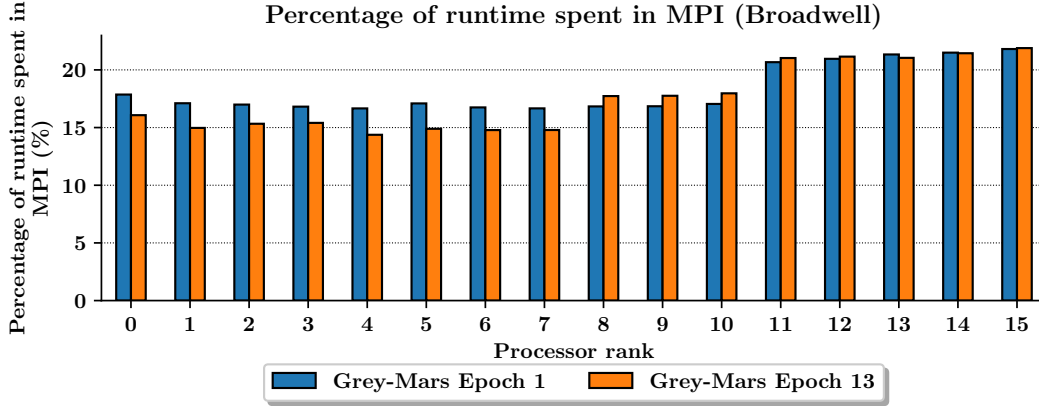
41

Fig. 7.12: Percentage of runtime spent inside the MPI library for each processor rank for the Grey-Mars configuration. Epoch 1 refers to time steps completed from model days 1 - 30, and epoch 13 refers to time steps completed from model days 390-420. These time periods are when Mars is approximately at opposing points in orbit relative to each other.

When run the Broadwell compute node, processor ranks 0-7 spend less time on communication compared to ranks 8-15 for both epoch 1 and epoch 13 (Figure 7.12). However, for epoch 1 ranks 0-7 consistently spend more time in communication than the same ranks during epoch 13. Ranks 0-7 are therefore spending more time on compute at epoch 13 than epoch 1. In contrast, ranks 8-12 and rank 15 spend more time in communication at epoch 13 than at epoch 1 (Figure 7.12).

7.5.2 Conclusions and discussion

Load imbalance refers to an uneven distribution of work across compute resources. In the domain of HPC it affects the performance of parallel codes only. For Isca, the large variation in MPI time observed across processor ranks suggests that the model suffers from a significant load balancing issue, which is amplified by the large portion of runtime that is spent inside calls to MPI.

Many of the subroutines found in Isca with long execution times inherently involve expensive communication. For example, when calculating global sums over 2D fields, each processor gathers the missing pieces of data they require to construct the global field from all other processes using blocking communication [64]. As Isca operates on a global domain, these points of synchronisation are unavoidable as communication must finish between all processes before the program can continue. Subroutines like this are found all throughout the Isca code, and each contributes to the large amount of time the model spends on communication. Unfortunately, Isca has been built around these points of synchronisation, and optimisation is not possible by using asynchronous message passing without affecting the scientific validity of the model.

The Grey-Mars simulation exhibits more severe symptoms of load imbalance. As discussed in Section 6.1.2, some radiation models can suffer from a load-balancing issue whereby calculations take longer on the side of the planet facing the Sun [76]. To test for this, the MPI communication times were measured at the first epoch (epoch 1), and then at the midway point of the planets orbit of the Sun (epoch 13) (Figures 7.12 and 6.1). Isca's communication pattern does not change depending on the epoch of the simulation. However, it was found that the same ranks consistently had different communication times at epochs 1 and 13, suggesting that the computational load changes as the simulation progresses.

Referring back to Figure 7.10, the Held-Suarez configuration generally presents more consis-

tency amongst its processors than the Grey-Mars configuration, which is to be expected as the forcing component of the model means that the calculations are more consistent on each rank. Although some variation was measured in MPI time across processor ranks for the Held-Suarez model configuration, this can be attributed to environmental variables outside the control of the experiment.

Much greater communication times were observed for the Sandy Bridge processor compared to the Broadwell processor. This is consistent with the findings of experiment A, whereby greater communication times were measured on Sandy Bridge. Although this does not determine the cause of this issue, it demonstrates that the large communication times are also found on single-node configurations, and are only exaggerated by internode communication.

7.6 Experiment F: Runtime variation

This experiment measured the differences in runtimes for each individual epoch comprising an Isca simulation.

7.6.1 Results
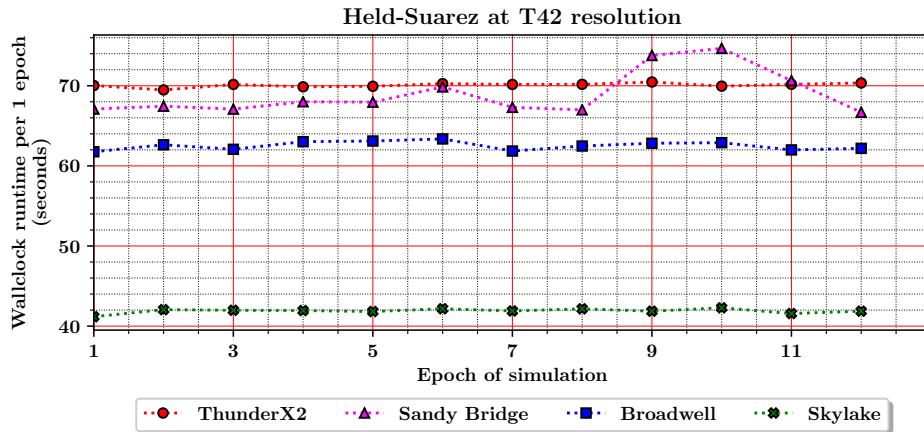
Fig. 7.13: Variation in runtimes for the Held-Suarez configuration running at T42 resolution.

For the Held-Suarez model configuration the runtimes for individual epochs have a range of 0.99 seconds, 1.11 seconds and 1.60 seconds for the ThunderX2, Skylake and Broadwell processors, respectively (Figure 7.13). However, the Sandy Bridge processor had more fluctuations in runtime throughout the full simulation with a range of 7.97 seconds.

The Grey-Mars simulation presents similar results, showing only minor variations in epoch runtime across all processors except Sandy Bridge (Figure 7.14). There is a large peak for the computation time of the Sandy Bridge processor at epoch 18, however rerunning this experiment causes peaks at seemingly random intervals.

7.6.2 Conclusions and discussion

The FMS manual warns of a spin-up time that can slow the performance of the first epoch of a simulation due to the initialisation of the global starting state [15]. This effect has not been
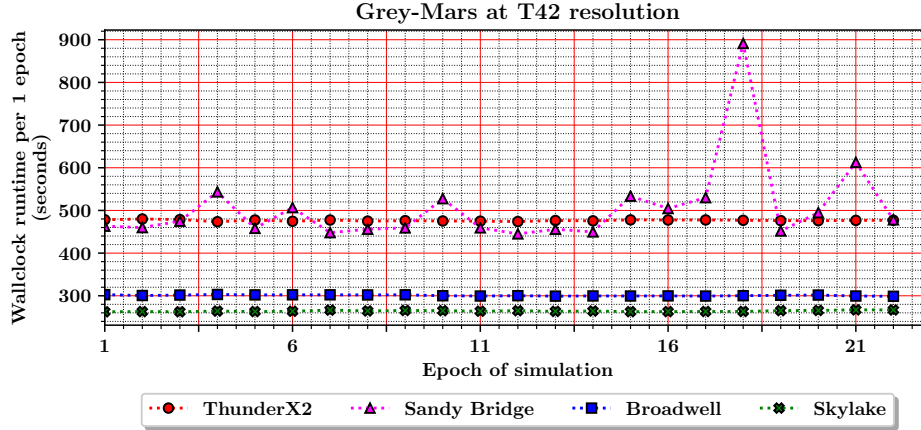
Fig. 7.14: Variation in runtimes for the Grey-Mars configuration running at T42 resolution.

observed in either the Held-Suarez or Grey-Mars model configurations, even in simulations that have not been visualised in Figures 7.13 and 7.14. The FMS manual was written in 2002 when the clock speeds of high performance processors were in the range of 1.1 GHz to 1.5 GHz, and memory-bandwidth rarely exceeded 1,600 MB/s [84, 85]. Perhaps the spin-up cost is now negligible when the model is run on more powerful hardware.

The runtimes observed on the ThunderX2, Broadwell and Skylake processors indicate that each epoch contains the same amount of work and no part of the planetary orbit is more computationally expensive than others. The results obtained on the Sandy Bridge processor are consistent with the erratic behaviour observed in other experiments, and therefore the results collected on this compute node can be treated as an outlier.

7.7 Experiment G: Roofline model analysis

The Held-Suarez simulation running at the T42 resolution delivers an operational intensity of 0.11 FLOPS/Byte and a double-precision floating point performance of 1.54 GFLOPS (Figure 7.15). This indicates that the configuration is limited by memory-bandwidth, as the program total performance is located underneath the DRAM ceiling. The Grey-Mars configuration presents a floating point performance of 1.96 GFLOPS, with the same operational intensity as the Held-Suarez configuration. Intel Advisor suggests that the peak double-precision floating point performance of a code running on the Skylake architecture using SIMD is 584.99 GFLOPS. This means that the Isca code is only running at 0.26% of the peak performance available on the hardware.

7.7.1 Conclusions and discussion

In addition to quantifying the performance of Isca, Figure 7.15 identifies 2 compute kernels referred to as Loop x and Loop y, for optimisation. Loops x and y are both found in Isca's FFT code and provide especially poor floating-point performance of 0.22 GFLOPS and 0.14 GFLOPS, respectively.

As discussed in Section 2.1.2, spectral climate models use a FFT to transform data between the spacial and frequency domains. Isca does this using the `fft991` subroutine, found in the `fft99.F90` module. This subroutine is used to perform multiple one-dimensional FFTs in succession over a two-dimensional array of sequential data when converting from a grid-point de-
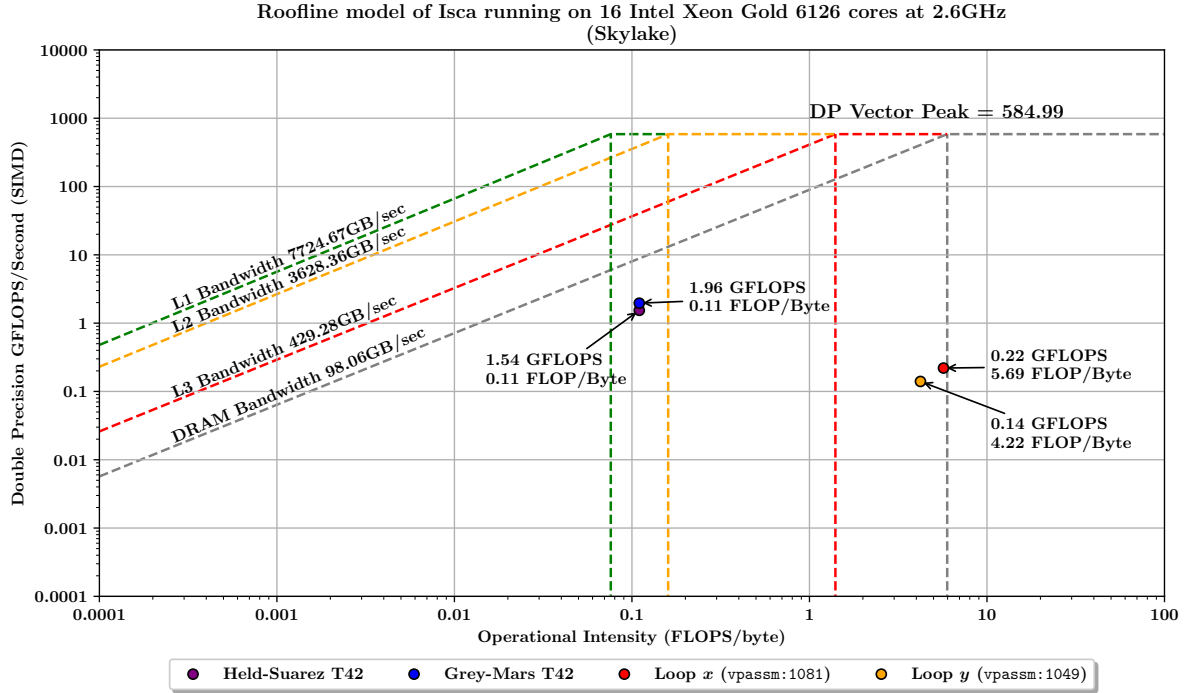
Fig. 7.15: Roofline model of the Isca code running on 16 cores of two Intel Xeon Gold processors at 2.6 GHz.

composition to the frequency domain and vice versa. This implementation of the FFT is known as Temperton's FFT, and has been adapted from a Fortran77 code written by Clive Temperton in 1981 [86]. The original source code of this implementation can be found in the deprecated EMOSLIB library by The European Centre for Medium-Range Weather Forecasts [87].
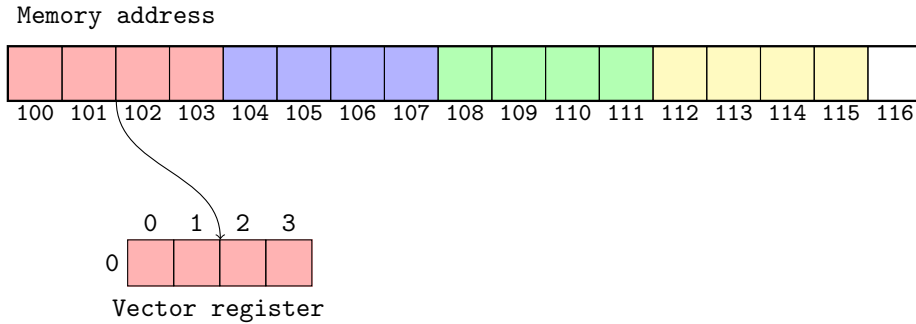
(a)

Although the `fft991` subroutine includes preprocessor directives to ignore vector dependencies at the most time-consuming loops neither the Cray, GNU or Intel compilers will perform automatic vectorisation. This results in four loops in the `fft99.F90` module being run as scalar code, even when vectorisation is possible. Intel Advisor indicates that this is caused by a fixed-width iteration through multiple data structures using a non-contiguous stride, as visualised in Figures 7.16a and 7.16b. In the case of the 256-bit wide vector registers found in BCP4's Broadwell processors, eight consecutive floats, or four consecutive doubles, may be loaded from memory with a single AVX-2 instruction. However, if the memory locations are not adjacent then they must be loaded using multiple instructions, negating the benefit of vector registers.

When forcing the compiler to use SIMD instructions for loops x and y by using the `!DIR$ VECTOR`

Memory address

Vector register

(b)
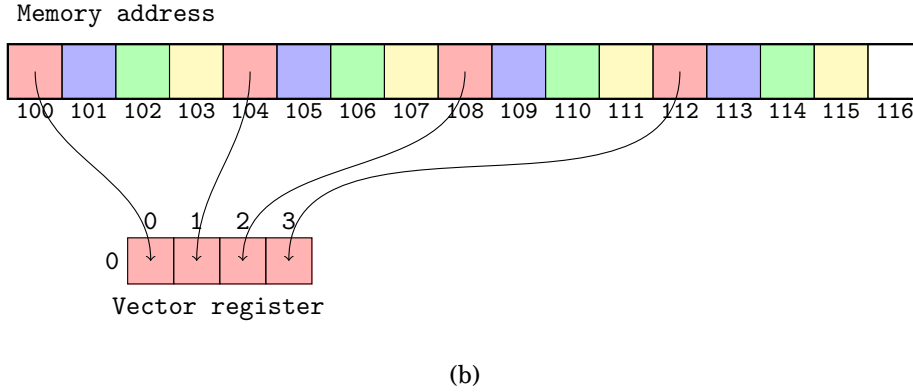
Fig. 7.16: (a) demonstrates that four contiguous single-precision floating point numbers can be read from memory with a single AVX-2 instruction, whilst (b) shows how four separate loads would be required for the same operation for non-contiguous data with a stride of 4.

Table 7.1: Runtime spent inside two compute kernels for both scalar and vector code.

Loop	Scalar time (milliseconds)	Vector time (milliseconds)
(x) `vpassm:1081`	822.5	649.8
(y) `vpassm:1049`	793.6	459.8

`ALWAYS` preprocessor directive there is only a marginal performance improvement over the scalar code, (Table 7.1). This supports the hypothesis that the code has not been written to vectorise on modern hardware.

Another issue regarding Temperton's FFT is that it performs the transformation in place. Although this reduces memory consumption, it introduces additional algorithmic complexity as the results of intermediate calculations are not written to a temporary array. This may have been important in the late 80s and early 90s when memory was in short supply, however modern processors often have in excess of 18 MB of on-chip cache and reducing memory consumption in this case is not a priority.

7.8 Summary

The main observations of all experiments are summarised:

Scalability For the T21 and T42 resolutions, the Skylake processor presents the best level of single-node performance. However, the large core count of the ThunderX2 allows for the best level of single node performance at the T85 resolution. Additionally, the ThunderX2 generally provides the best level of scaling relative to serial performance.

Load balancing A serious load balancing issue has been discovered, whereby between 15-40% of the program runtime is spent inside MPI. Although communication is the biggest performance limiting factor of the code, all identified points of synchronisation are unavoidable, and cannot be optimised without rewriting the entirety of the model. Additionally, there is evidence to show that some processor ranks have a higher computational load depending on the epoch of the simulation. This could be caused by larger levels of radiative heat transfer on different ranks as the simulation progresses.

Vectorisation As Isca operates on double-precision floating point values, the small vector reg-

isters of the ThunderX2 cannot be used on complex numbers. This also affects the performance of the Intel processors, as vectorisation only accounts for a performance gain of between $1.02\times$ and $1.25\times$ the scalar code.

Compilers On the Intel machines ICC outperforms GCC in all cases. However, on the ThunderX2 GCC provides better performance than CCE. These results were used to inform the choice of compiler for all other experiments.

Slow FFT Isca uses a FFT that was written in 1981 and it has been demonstrated that some of this code does not automatically vectorise. Only insignificant performance gains are observed when forcing the code to use SIMD registers, and it has been determined that this is an area of the code that can be optimised.

CHAPTER 8

This chapter builds upon the findings presented in chapter 7 by describing the design and implementation of two performance optimisations, *A* and *B*. Optimisation *A* utilises the FFTW library in place of Temperton's FFT, and optimisation *B* uses single-precision floating point numbers.

8.1   Optimisation *A*: Fast Fourier Transform

Although it may be possible to rewrite Temperton's FFT to efficiently use vector registers, this would be a time-consuming task and does not guarantee a performance improvement. Therefore, the Isca codebase has been modified to allow for the use of the open source FFTW library instead.

8.1.1   Implementation

In order to call FFTW rather than Temperton's FFT, a new Fortran module `fftw.F90` has been written. Preprocessor directives have been added to the existing `fft.F90` file to allow for the type of FFT used by Isca to be selected at compile time. Compiling the model with the `-DFFTW3` preprocessor directive will compile the model to use FFTW instead of the default call to Temperton's FFT. Isambard, BCP3, BCP4 and BP have module files that allow for automatic linking to the FFTW library. If using the library on other systems the FFTW library must be installed and linked to Isca manually. FFTW provides both a single and double-precision version of its library, with subtle differences to the names of the interfaces it provides. Preprocessor directives must be used to choose which version of FFTW is linked to the Isca code at compile time.
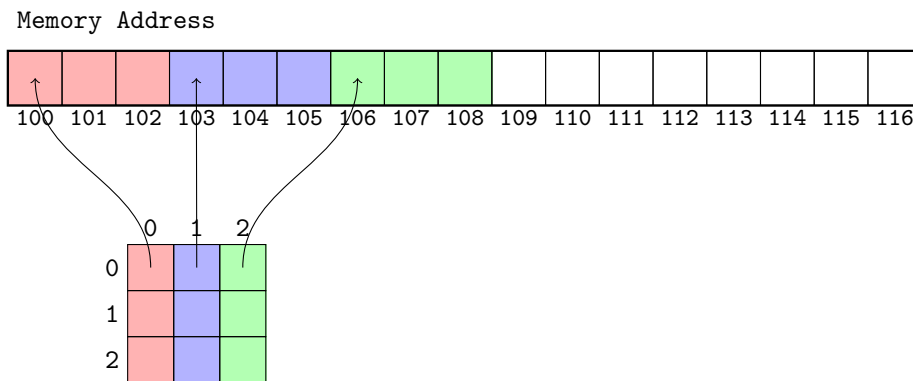
Fig. 8.1: Contiguous data layout in memory for a two-dimensional array in Fortran.

To guarantee proper data alignment for SIMD utilisation, the data structures on which the FFT is applied are allocated using the `fftw_malloc` subroutine and deallocated using the `fftw_free` subroutine, both of which are provided by the FFTW library [33]. These subroutines have the same behaviour as the `allocate` and `deallocate` subroutines found in the Fortran standard library, however they also call `memalign` to ensure that the data structures are properly aligned

[34]. Figure 8.1 shows contiguous aligned memory for a two-dimensional array in the Fortran programming language, which uses a row-major order for multidimensional array storage [88].

Isca computes the DFT of sequences of both real and complex numbers. A one-dimensional transform from a real array of size N results in a complex array of size $N/2$. When implementing this using FFTW, the same input and output arrays are reused for multiple transforms to take advantage of the FFTW plan data structure. As FFTW computes an unnormalised DFT, the result is multiplied by the number of items in the input sequence. This means that the result must be scaled by a factor of $1/N$ after the DFT is calculated, which adds a small overhead to compute costs in addition to the cost of the DFT.

Additional overhead costs are incurred when populating the input array for which the DFT will be calculated. Fortran is a pass-by-reference language, which means that arguments are passed to subroutines as a pointer. Before the DFT can be calculated the input array must be populated with the data from the array passed to the wrapper subroutine. Although this involves only one iteration though the array, this can accumulate to a significant amount of runtime when many FFTs are called in succession.

8.1.2 Verification of results

To ensure that FFTW computes the same values as Temperton's FFT, both forward and backward transforms were tested on sequences of known data. The results of this test show that both transforms compute the exact same DFT and IDFT for 30 unique sequences of data. Additionally, computing both the DFT and IDFT of a sequence in succession yields the original sequence upon which the transforms were applied.

8.1.3 Performance analysis

Methodology

The time taken to complete a number of one-dimensional FFTs was measured for both FFT implementations in order to compare the performance of FFTW against Temperton's FFT. Each FFT implementation was tested on four different sizes of randomly initialised two-dimensional data structures, similar to those found in Isca. For example, a two-dimensional array of size 128×64 will compute the DFT of 128 one-dimensional arrays of size 64. The sizes of the arrays tested correspond to the different array sizes used for the T21 (64×128), T42 (128×64), T85 (256×128) and T170 (512×256) model resolutions. To emulate the Isca code the test program was compiled using the same compiler flags used to compile Isca. Experimental error was accounted for by computing the mean value of 100 transformations, improving the accuracy of findings and reducing the impact of anomalies.

Results

The performance of both the Sandy Bridge and Broadwell processors improves linearly with the size of the data structure on which the transform is applied (Figure 8.2). The performance of the ThunderX2 and Skylake processors sharply rises when run on a problem size of 256×128 and 512×256, although only marginal performance gains are observed for the smaller problem sizes. The greatest performance improvement was observed on the Sandy Bridge processor when performing a FFT on a grid size representing the T170 resolution. For this configuration the
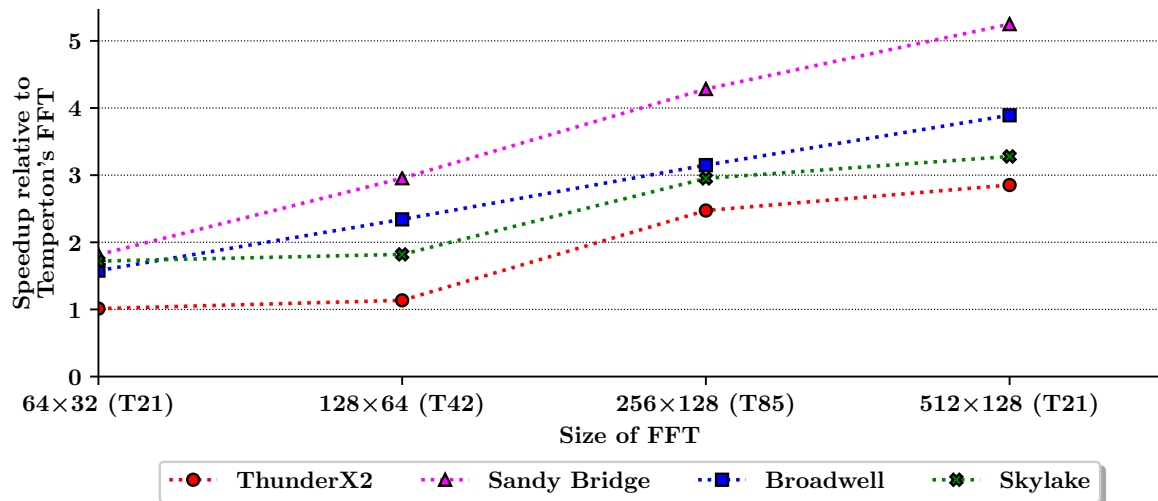
Fig. 8.2: Speedup of FFTW relative to Temperton's FFT.

FFTW code ran 5.25× quicker than Temperton's FFT, and in all cases the largest problem size saw the greatest performance speedup over Temperton's FFT.

The ThunderX2 had the lowest performance across all problem sizes, and only significant performance gains were observed for problem sizes greater than T42 (Figure 8.3). The Intel processors saw the best levels of performance, likely due to the FFTW library originally being written for x86-64 processors.
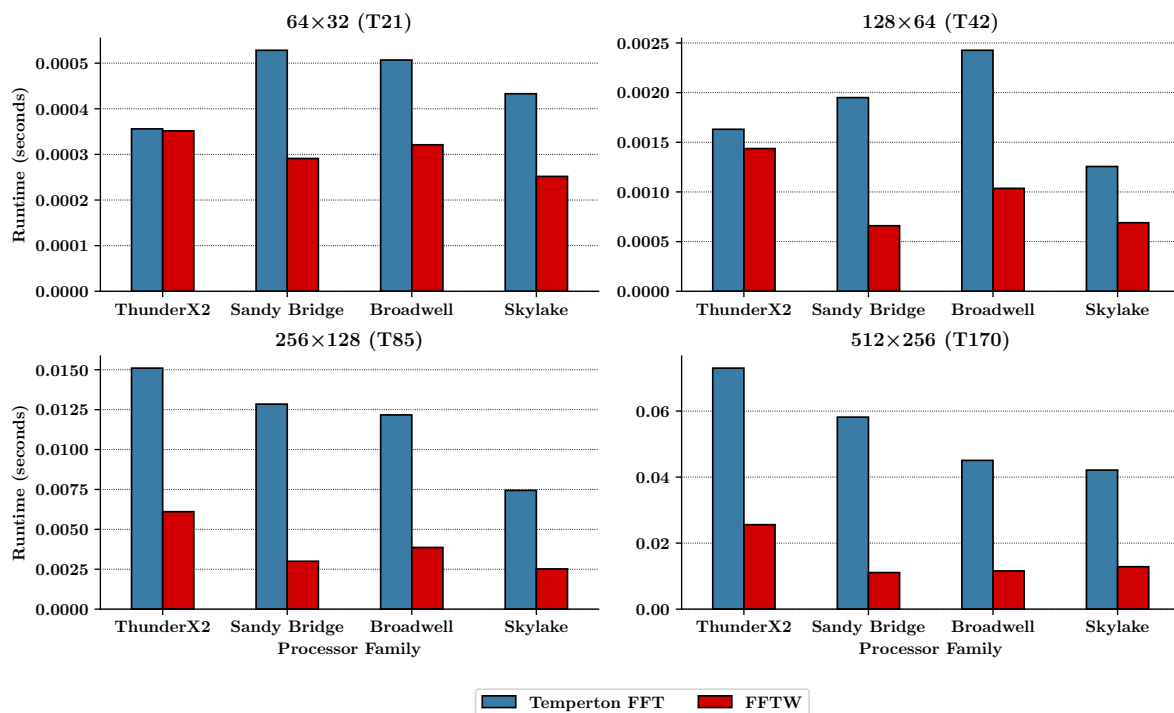
Fig. 8.3: The performance of Temperton's FFT compared to the performance of FFTW across multiple domain sizes.

Conclusions and discussion

Principles of software engineering recommend that code should be modular by design, which means that software components should be separated according to functionality [89]. Using a library to perform the FFT adheres to this principle and allows for future updates to the library to benefit the performance of Isca. Due to the popularity of the FFTW library, it is under constant development to allow for the utilisation of the latest hardware features, whilst remaining compatible with older systems.

8.2 Optimisation B: Single-precision floating point numbers

Both x86-64 and AArch64 processors perform scalar floating point arithmetic in 64-bit registers, and therefore the time taken to perform floating point arithmetic on a single data item is approximately the same for both single and double-precision variables [82, 90]. At a larger scale, single-precision arithmetic can improve overall system performance by reducing RAM, cache, and memory bandwidth consumption, in addition to more efficient usage of vector registers [68].

By default, Isca uses double-precision floating point variables to store all atmospheric variables. As double-precision complex variables in Fortran use 128-bits of memory, SIMD instructions cannot be applied to operations over complex data structures using SSE or NEON registers. To enable complex variables to fit into these registers, Isca has been compiled to use single-precision floating point numbers, halving the memory consumption of complex variables to 64-bits.

8.2.1 Implementation

The Isca code contains existing infrastructure to allow for the default size of real and complex variables to be selected at compile time as the codebase includes interfaces to both single and double-precision versions of subroutines. To change the default size of real and complex variables in the model, a number of preprocessor directives and compiler flags can be specified at compile time to allow for subroutine overloading. This changes the kind of variables declared using the `MPP_TYPE_` macro, which is used throughout the codebase to specify the default kind and type of dummy arguments.

8.2.2 Performance analysis

Methodology

The wallclock runtime of the single-precision version of Isca running both the Held-Suarez and Grey-Mars configurations was measured, allowing for comparison with the double-precision version. Additionally, the operational intensity (FLOPS/Byte) and floating point performance (GFLOPS/s) was remeasured for a single epoch of the program executable. This allowed for a new roofline model to be plotted to visualise how the performance limitations of the code changed. To determine if single-precision variables utilise SIMD registers more efficiently, the runtime of the single-precision version of the model was measured with and without vectorisation enabled.

Results
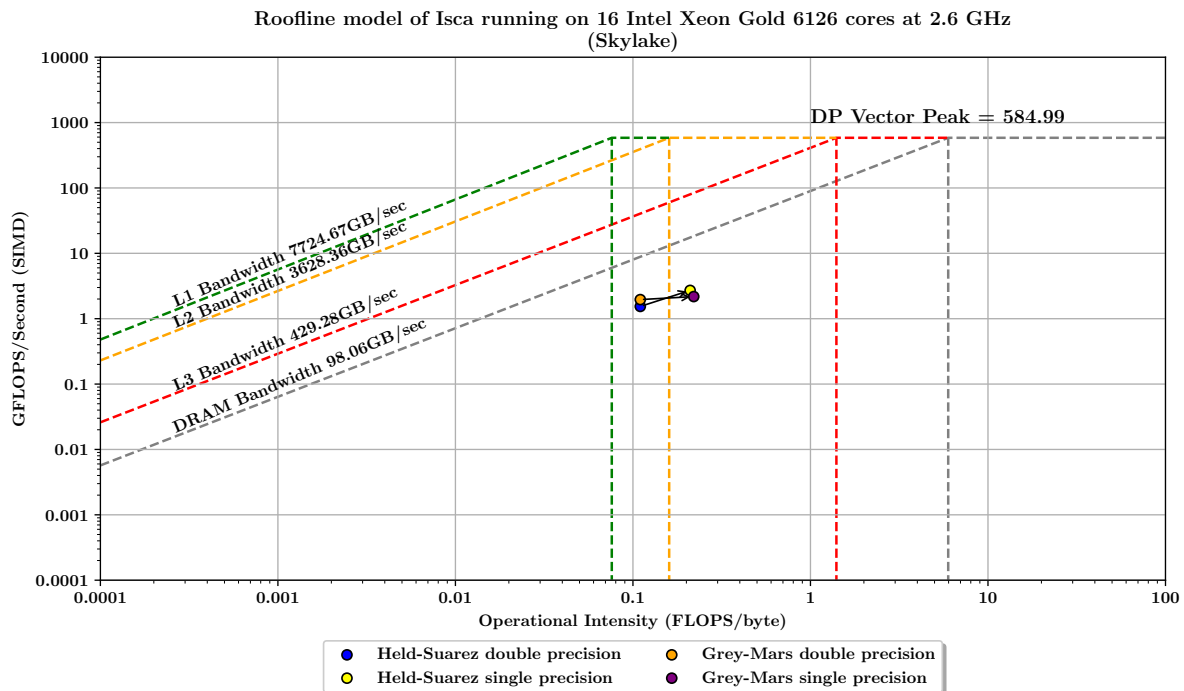
Fig. 8.4: Roofline model comparison of the single and double-precision versions of Isca running the Held-Suarez and Grey-Mars model configurations.

Using single-precision floating point variables, the operational intensity increased from 0.11 to 0.21 for the Held-Suarez configuration, and 0.11 to 0.22 for the Grey-Mars configuration (Figure 8.4). Additionally, the floating point performance increased from 1.54 GFLOPS to to 2.71 GFLOPS for the Held-Suarez configuration and from 1.96 GFLOPS to 2.18 GFLOPS for the Grey-Mars configuration.
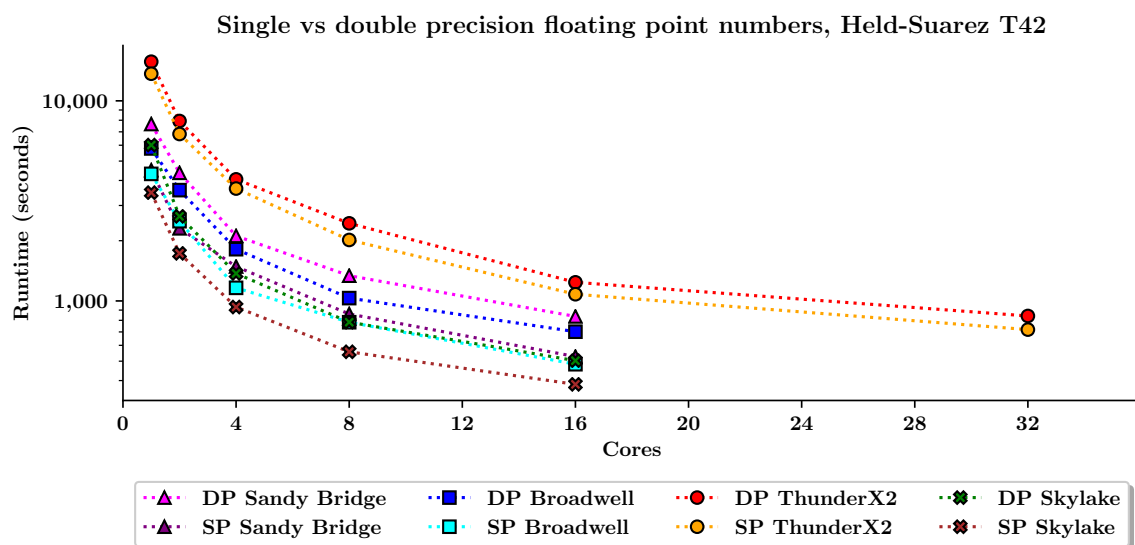
Fig. 8.5: Comparison of the wallclock runtimes for single and double-precision floating point numbers for the Held-Suarez configuration running at T42 resolution.

Single-precision arithmetic is significantly faster than double-precision arithmetic at all core counts (Figure 8.5). There is no relationship between the level of performance improvement and number of concurrently utilised processor cores, suggesting that the speed of MPI communication is not significantly affected by decreasing the precision of variables.
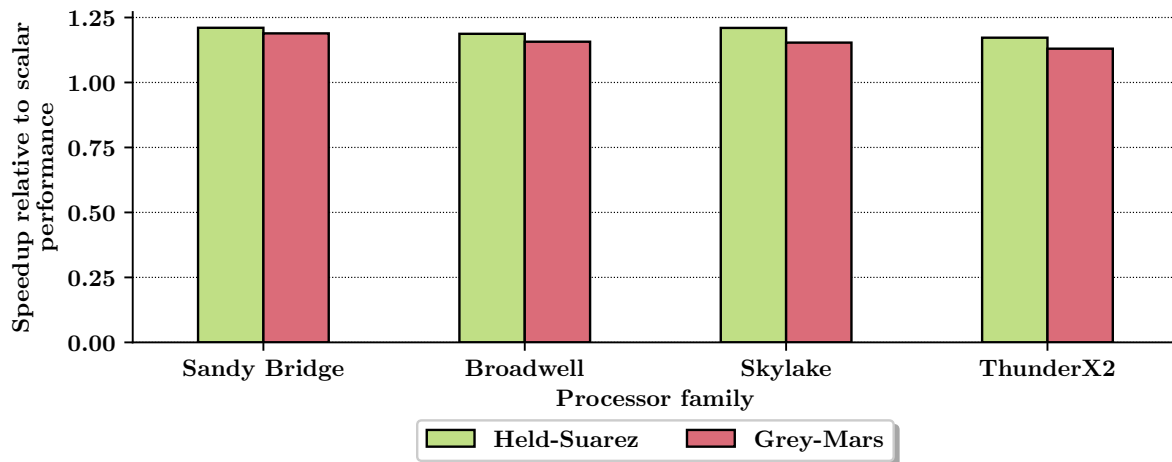
Fig. 8.6: Speedup of the vectorised code relative to scalar.

When using single-precision floating point numbers, vectorisation accounts for an approximate 1.18× speedup of the scalar code (Figure 8.6). In comparison, vectorisation for double-precision floating point numbers only accounts for a 1.09 × speedup (Figure 7.8). This indicates that vectorisation is more efficient when used on single-precision variables. Vector reports produced when compiling the code confirm this, as they show that SIMD instructions can now perform operations over complex data structures across all processor architectures, including the ThunderX2.

8.2.3   Conclusions and discussion

Isca is currently used to research the climate behaviour of exoplanets of which very little is known of atmospheric conditions, and therefore results of these simulations are expected to be imprecise. To account for this, Isca calculates the global means of atmospheric variables to be used as approximations, and for this use-case single-precision variables are adequate.

Meteorologists typically use a brute-force approach to model parameter selection, whereby many different simulations are run with only slight variations to parameter settings. The use of single-precision variables would be useful in this situation, as more parameter configurations could be tested in the same amount of time. Parameter settings that produce interesting results can be rerun using double-precision variables at a higher resolution.

8.2.4   Verification of results

In the Fortran 90 standard, single-precision real numbers have 7 digits of accuracy, and double-precision real numbers have 15 digits of accuracy. Because of this, the units of last place numerical analysis technique cannot be used to compare single and double-precision outputs. To verify the scientific validity of the results, both single and double-precision output files were given to domain experts for comparison.

8.3 FFTW with single-precision variables

8.3.1 Performance analysis

Methodology

The wallclock runtime of the code using both optimisations was measured and compared against optimisations A, B and the unmodified code. FFTW provides both a double and single-precision version of its library, so it remains compatible with Isca when compiled to use single-precision variables by default.

Results
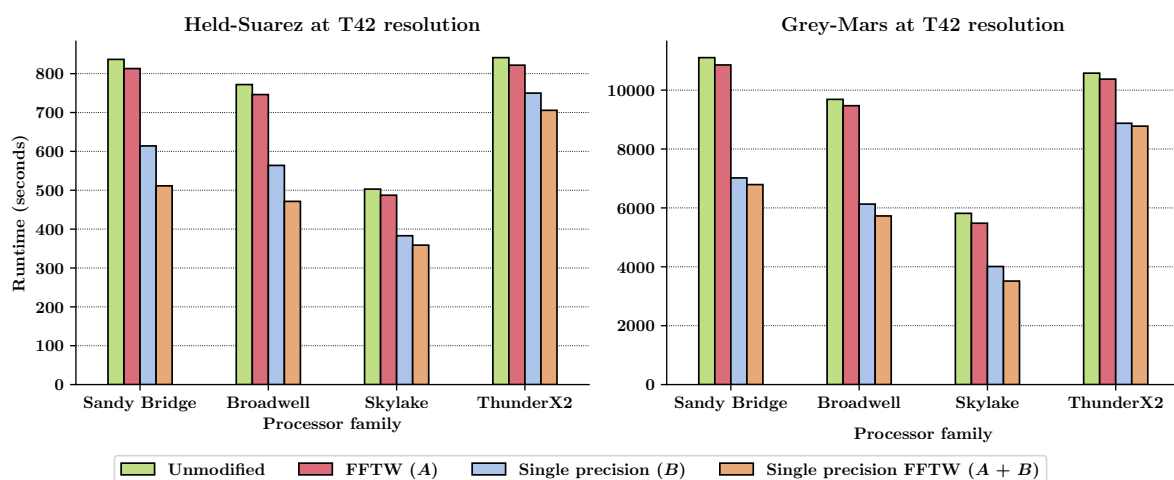
Fig. 8.7: Performance comparison of the Held-Suarez and Grey-Mars configuration at T42 resolution when using different performance optimisations.
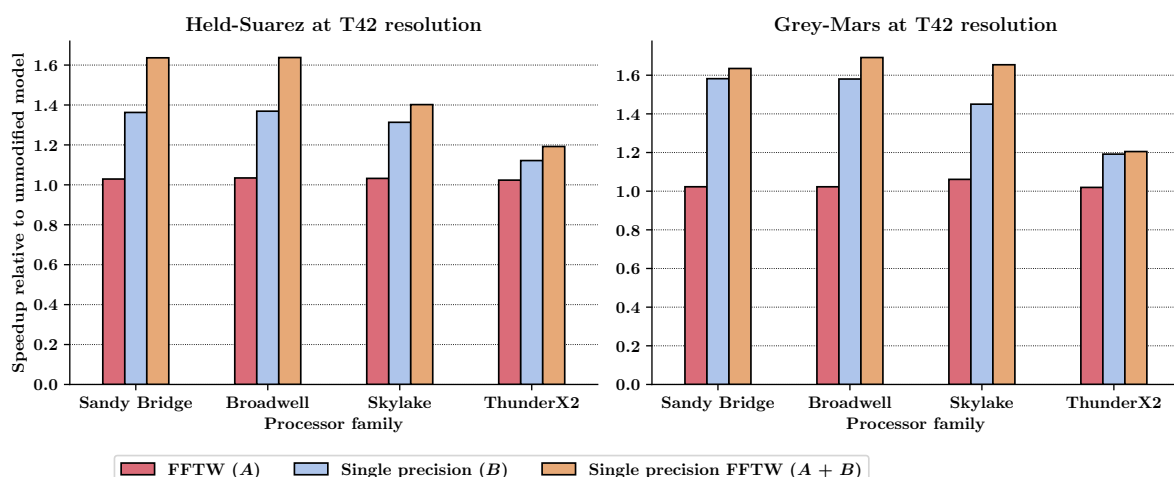
Fig. 8.8: Speedup of performance optimisations relative to the unmodified model.

The Skylake node provided the best overall performance for the fully optimised model, with a mean wallclock runtime of 358.8 seconds for the Held-Suarez configuration, and 3,515.7 seconds for the Grey-Mars configuration (Figure 8.8). These runtimes correspond to a speedup of 1.40×

and 1.65× relative to the unoptimised code, respectively. The ThunderX2 presents the worst performance, providing a mean wallclock runtime of 705.7 seconds for the Held-Suarez configuration and 8,776.4 seconds for the Grey-Mars configuration. It also provided the smallest performance speedup of 1.19× and 1.20× the unoptimised code for the Held-Suarez and Grey-Mars configurations, respectively.

Conclusions and discussion

The code responsible for performing the FFT in Isca only accounts for approximately 5-10% of the total compute costs of the model, depending on the model configuration. Although FFTW runs 5× faster than Temperton's FFT in some cases, the overall performance improvement to Isca is minor. However, when the FFTW library is used together with single-precision variables there is a synergistic effect, resulting in an even greater overall performance gain then when either optimisation is used alone.

8.4 Conclusions

This chapter presented two performance optimisations, demonstrating runtimes up to 1.65× faster than the unmodified model on a Skylake node. Additionally, the findings from this chapter suggest that bespoke high-performance code does not improve over time, and that specialist libraries should be used when possible as they are usually kept up to date with modern hardware developments.

Despite the improvement of the FFT, there is very little scope for optimisation without addressing the deeper rooted problem of the MPI imbalance discussed in Section 7.5. Although the use of single-precision floating point numbers did improve the performance of the model, this was not because of reduced communication times between processor ranks. Optimising the MPI communication would require a total redesign of the model, and may be not possible to do using a distributed-memory programming model such as MPI.

Using the results from the experiments carried out in Chapter 7, the performance of Isca has been projected to Fujitsu's A64FX Arm processor, which is planned to be debuted in the Post-K supercomputer in 2021 [91]. Most notably, it will be the first production processor to use the new Arm SVE instruction set architecture, which allows for SIMD operations using 512-bit vector registers. Estimating the performance of unreleased hardware is challenging as manufacturers often release optimistic performance estimations to generate interest in their devices.

This chapter aims to use the literature published by Fujitsu to estimate the raw performance of of the A64FX processor. This information is then used to project the performance of Isca to the A64FX using a simple performance model based on Amdhal's law [92].

9.1 Hardware performance estimation

Table 9.1: Hardware comparison of the Cavium ThunderX2 and Fujitsu's A64FX. As the A64FX is under development, this information is subject to change.

Feature	ThunderX2	A64FX
Instruction set architecture (base)	Armv8.1	Armv8.2-A
Instruction set architecture (extension)	NEON	SVE
Clock speed (GHz)	2.1	1.7 - 1.9 (est)
Number of cores	32	48 + 4
SIMD width (bits)	128	512
Floating point performance (GFLOPS)	537.6	2,688
Memory bandwidth (GB/s)	240	1024

9.1.1 Floating point performance

Using Equation 4.1, a dual socket configuration of the A64FX is calculated to provide a theoretical peak floating point performance of 2,688 GFLOPS, which is a 2,150.4 GFLOP improvement over the ThunderX2. This estimation has been calculated assuming that all operations are performed using the full width of the 512-bit vector registers, which is highly unlikely for real applications.

The A64FX is expected to have a low clock rate of between 1.7-1.9 GHz. This is much lower than the Skylake processor, which must decrease its clock speed when using its 512-bit vector registers. It is not unreasonable to assume that the A64FX will not implement dynamic frequency scaling as the base clock rate is already low.

9.1.2 Memory-bandwidth

When announced, Fujitsu claimed that the processor will deliver a peak memory bandwidth of 1024 GB/s (Table 9.1) [91]. STREAM TRIAD results can expect to achieve 80% of peak perfor-

mance, resulting in a functional memory bandwidth of 819.2 GB/s.

9.2 Isca performance estimation

To estimate performance of Isca on the A64FX, it is important to consider only the performance of the ThunderX2 processor, as it is the only processor tested in this study that uses the Armv8 instruction set architecture.

9.2.1 Scalar estimation

The degree to which the number of processor cores affects the runtime of a parallel code can be calculated. In 1967, Gene Amdahl proposed Amdhal's law, which governs the theoretical speedup in latency of a code when run in parallel [93]. It states that the theoretical speedup of a parallel task (S) is dominated by the fraction of the task that must run in serial (p). It is formally expressed in Equation 9.1.

$$S(n) = \frac{1}{(1-p) + \frac{p}{n}} \tag{9.1}$$

To estimate performance, we must first calculate the amount of speedup possible applied to the proportion of the code that can benefit from additional compute resources $\frac{p}{n}$. This can be done using non-linear least squares regression by treating Amdhal's law as an objective function of speedup. This method calculates the parallel fraction of the code as $p = 0.9776 +/- 0.0011$ (Figure 9.1).
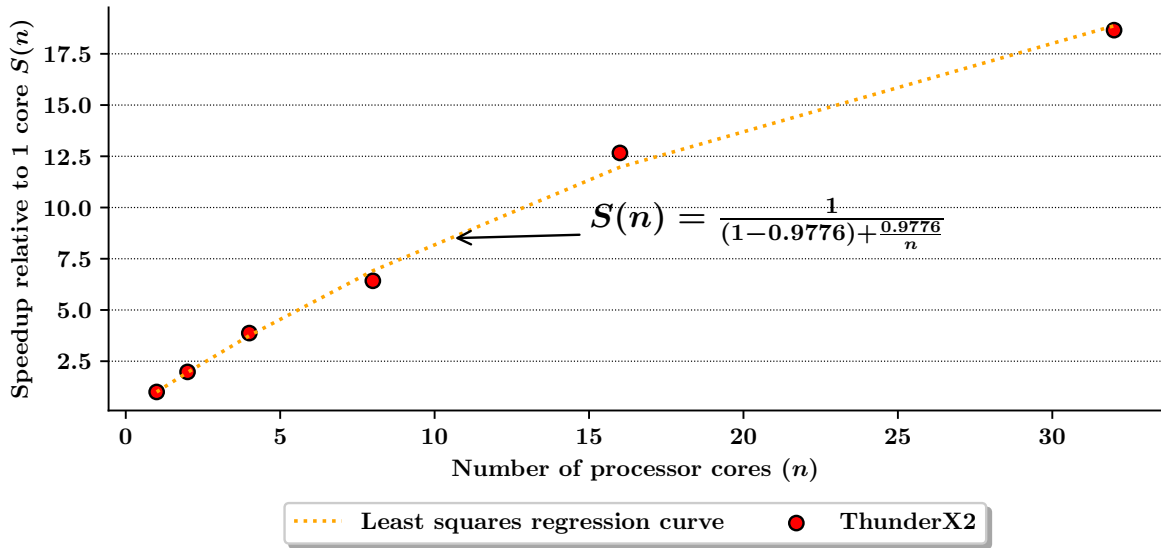
Fig. 9.1: Non-linear least squares regression applied to the speedup of the scalar ThunderX2 code relative to one processor core.

To estimate the performance of a processor, the number of effective cores e utilised to run the code in parallel must be calculated using Equation 9.2, whereby m refers to the maximum number of cores on the processor.

$$e = \frac{1}{(1-p) + \frac{1}{m}} \tag{9.2}$$

We then calculate the scalar floating point performance of the processor. Assuming a base clock frequency f of 1.8 GHz for the A64FX, the number of floating point operations can be estimated to be $G_T = 59.47$ for the ThunderX2 and $G_A = 59.59$ for the A64FX (Equation 9.3).

$$G = f \cdot e \tag{9.3}$$

The wallclock runtime of the A64FX, R_A can be estimated using the floating point performance of both the ThunderX2 and A64FX, and the measured runtime of the ThunderX2 R_T at each core count (Equation 9.4).

$$R_A = \frac{G_T}{G_A} \cdot R_T \tag{9.4}$$

9.2.2 Vector estimation

Thus far, all calculations have used the unvectorised benchmark of the ThunderX2. The predicted wallclock runtime R_A must be adjusted to account for the 512-bit registers found in the A64FX. On the ThunderX2, the code compiled to use SIMD is on average 1.035× faster than the scalar code. We can therefore assume that the performance gain will be twice that for a vector width of 256 bits, and quadruple that for a width of 512 bits. Consequently, we can estimate that the A64FX will see between a 1.1× and 1.2× performance gain from the use of SIMD instructions and this can be applied to scale the estimate R_A. This estimate is reasonable, as the Isca code does not heavily rely on vectorisation for performance.

9.2.3 Results

It is estimated that Isca will run faster on the A64FX than the ThunderX2, providing an approximate 1.17× +/-10% performance speedup relative to the ThunderX2 at all core counts (Figure 9.2). This prediction is assuming that the code is compiled using the same flags and compiler as used on the ThunderX2. However, it is to be expected that there will be a new version of GCC by the release of the A64FX, which may produce better-optimised instructions for the Arm architecture.
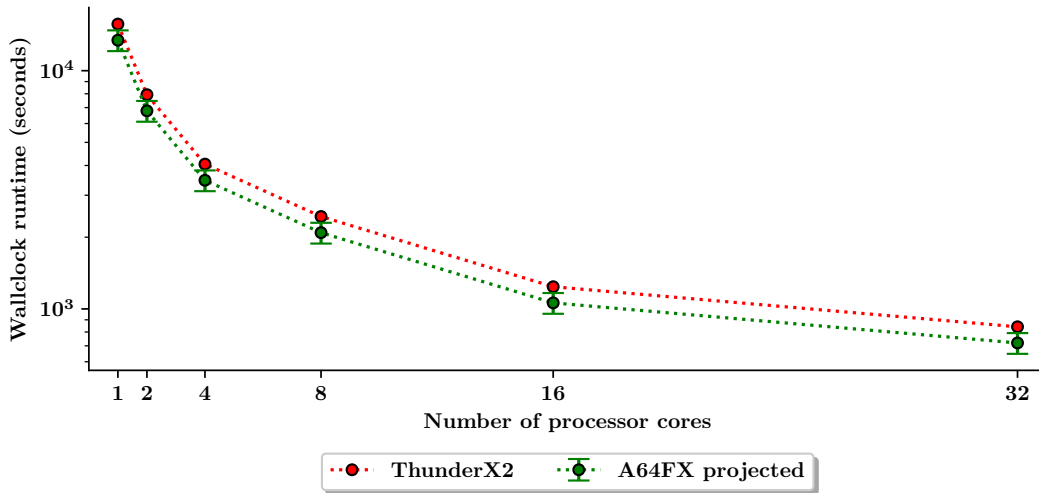
Fig. 9.2: Projected performance of the A64FX compared to the measured performance of the ThunderX2 running the Held-Suarez configuration at T42 resolution.

9.3 Conclusion

These estimates are more of a thought experiment than a methodical performance model of the Isca code, using only the clock speed and estimated vector gain of the processor into account. Perhaps a more rigorous performance model would also consider memory-bandwidth and cache efficiency. However, the estimates offer an interesting insight into the performance of the future of Arm server hardware running a production scientific code.

Part III

Reflection, Critical Evaluation and Conclusion

CHAPTER 10

Reflection

This chapter presents a reflection of the challenges encountered throughout the course of this research project.

10.1 The Fortran programming language

The initial challenge was learning the Fortran programming language, having not used it prior to this project. This was complicated further by the size and complexity of the Isca codebase, which made it difficult to learn the language by example. Fortran behaves very differently from other more familiar programming languages like C and Python, and a long time was spent learning the intricacies of the language before any real development could take place. The process of learning the language involved writing many small toy programs to test the behaviour of different subroutines.

Despite the Fortran programming language first appearing in 1957, it is still used in the development of many high-performance codes, especially in the simulation of the physical sciences. Exposure to such a large Fortran codebase has developed a set of transferrable skills that can be used for other programming projects in the domain of HPC.

10.2 Compilation of the model

Prior to starting this project, no performance optimisations had been identified and there was no guarantee that the code could be optimised. This placed a lot of pressure on ensuring that the model could compile and run so that the project could progress onto benchmarking, and then performance optimisation. Simply compiling the model was a non-trivial process, and it took 4 weeks before Isca could compile and run on each cluster without crashing or hanging. There were many small problems with the codebase that were unique and difficult to research, and often required an obscure fix in the form of a compiler flag or environment variable. Using a range of compilers generated further problems, as different compilers caused the code to produce unique behaviours.

At the beginning of the project, a large amount of time was spent on compiling the model using CCE on the Isambard supercomputer. When tested, the executable produced by this compiler provided worse performance than GCC and was therefore not used throughout the rest of the project. With hindsight, this time may have been better spent identifying other performance optimisations, or using the Arm HPC compiler instead.

Isca is a very fragile codebase and even minor changes caused the model to crash. The main source of crashes throughout this project occurred as a result of atmospheric variables exceeding their expected range. The chaotic nature of the model meant that this was a frequent occurrence, as small changes to parameter values would cause vastly different results. Isca can sometimes take up to half an hour to compile, especially when using the CCE compiler. This proved to be challenging when implementing code changes, as minor mistakes sometimes required a total recompilation of the model, wasting a significant amount of development time.

Much of the FMS code does not strictly follow the Fortran standard, and relies heavily on compiler features that exist only to remain compatible with legacy codes.

Many issues occurred on the BluePebble supercomputer as the cluster was still in its beta phase of development throughout the duration of this project. Many of the fixes could not be performed by changes to the codebase, and required cooperation with the system administrators to change the configuration of the PBS module. One issue unique to this machine was caused by the overuse of stack memory, which resulted in segmentation faults when running the model at higher resolutions. Upon initialisation, Isca sets the amount of stack memory it requires, however BluePebble does not grant permissions to its users to allow for this to be done.

10.3 Data collection

The Python library written for data collection was invaluable as the volume of test runs that were required to collect accurate data would have been unmanageable to perform manually. Even when using this library, a large portion of all jobs submitted failed for various reasons. At the beginning of the project, it was a common occurrence for 9 out of 10 submitted jobs to fail. However as the project progressed, each cluster and configuration used its own submission script, so that the correct resources could be requested for each configuration. Although some jobs would still crash, this greatly reduced the rate of failure.

Additionally, the Python library allowed for the collected data to be visualised in the various graphs shown throughout this document. All trends and behaviours of the code were identified from the visualisation of data.

Critical evaluation and conclusion

This project aimed to present a comprehensive performance analysis and optimisation of the Isca climate model on multiple processor architectures. The following chapter assesses whether this has been achieved and discusses the limitations of the work presented.

11.1 Areas of improvement

Although this research project presents a grounded performance analysis of numerous high-performance processors, Isca is just one program and the performance of said processors cannot be judged based on this alone. Isca also has a relatively low computational intensity for a high-performance code, and did not push any of the processors tested to their limits. More computationally intensive programs like TeaLeaf, CloverLeaf, or other synthetic benchmarking codes would provide a better platform for performance comparison, as mentioned in Section 4.1 [94, 95].

The results presented in Chapter 7 may disproportionately represent the performance of the T42 resolution. The best performance of the ThunderX2 was observed at the T85 model resolution, however many of the experiments were performed at the T21 and T42 resolutions only. This may cause the ThunderX2 to be misrepresented, as the T21 and T42 resolutions could only utilise 16 and 32 out of the 64 cores available, respectively. This was unintentional, however providing benchmarks across all different combinations of processor, configuration and resolution was challenging to manage, and the T42 resolution was chosen as the default for many experiments. The time restrictions of the three-month project meant that it was simply not possible to collect results for all possible scenarios. In this project, the accuracy of results was prioritised over collecting inconsistent data for many experiments.

11.2 Conclusion

Whilst considering the scale of this project, the results support other evidence that indicates that the ThunderX2 processor delivers competitive levels of performance to that of modern Intel processors [3]. The ThunderX2 gave the best level of performance when running Isca at a high resolution (T85) and the cause of this was determined to be the large core count of the processor, which allowed for communication to stay within a single node. However, it was still outperformed by the Broadwell processor when running on two nodes.

To identify performance optimisations an extensive performance analysis of the Isca climate model has been presented. The main performance-limiting factor identified is a severe load-balancing issue, which causes up to 40% of the program runtime to be spent on blocking MPI communication. This results in a large cost for unavoidable points of synchronisation when performing global operations such as calculating means. This issue was exaggerated when running across multiple nodes, causing substandard levels of scaling for multinode configurations.

When a project is not constrained by time limits, optimisation efforts are typically focused on improving the greatest performance bottlenecks of a code [7]. However, optimising the MPI in

this case would be a significant feat of software engineering, requiring more time than available to three-month MSc project.

Although the main performance-limiting factor could not be optimised, considerable research was undertaken to identify, design and implement an optimisation to the FFT, which was the second most time-consuming part of the code. Isca performs a spherical FFT, which constrains the type of FFT that can be used. This required an extensive review of the literature regarding FFT algorithms before the correct type of FFT was identified in the FFTW library.

The outcomes of this project indicate that it has been successful. The Isca codebase has been ported to three new supercomputer clusters, one of which is now actively used by researchers at the University of Bristol. The meteorological research group at the University of Bristol has purchased a £10,000 dedicated compute node for the BluePebble supercomputer as a direct result of the work presented in this thesis. Additionally, 223 compute nodes on BCP3 and 168 compute nodes on Isambard can now be utilised by users of Isca. This project has also resulted in contributions to an open source codebase that is actively used for research. An additional unplanned outcome of this project was the performance projection of Isca to the A64FX processor using a simple performance model based on Amdhal's law.

11.3 Further work

11.3.1 Scaling

At the resolutions commonly used by Isca, the code does not scale outside of a single compute node. This raises questions as to why the model was written to use MPI, instead of a shared-memory programming model such as OpenMP. When the FMS was under development in the 1990s, compute nodes typically consisted of only one or two processor cores, which means that large scale MIMD parallelism would only be possible using MPI. As the number of processor cores per node have increased, perhaps an OpenMP port of the code would be viable. Although this would not completely remove the need for points of synchronisation, it would negate the cost of operations like global broadcasts, which could be executed without direct message passing.

The work presented in this thesis measured spatial resolutions up to and including T85 only. Isca officially supports resolutions up to T170, however it would be trivial to modify the Python library to allow for simulations of arbitrary granularity. Larger resolutions would allow for the model to be run across 10s of nodes rather than just the maximum of three used in this project. Although this is non-standard and does not represent how the model is used by researchers, it would be interesting to study how the model responds to greater levels of parallelism. However, the results of this project suggest that the additional cost of communication would outweigh the benefits of additional parallelism. Higher resolutions would also allow for the ThunderX2 processor to be tested in a multinode configuration, which was not investigated as part of this study.

Unpredictable behaviour was observed on the Sandy Bridge compute nodes (BCP3), whereby there were large fluctuations in the runtime of simulation epochs, and internode communication times were much larger than single node times. Whilst some interpretation of this has been explored, no definitive cause was identified. However, it is likely that the poor performance is as a result of congestion on a heavily loaded cluster, or an issue with networking. These hypotheses could be explored by further synthetic benchmarking.

11.3.2 Comparison with other models

The performance of Isca could be measured relative to the performance of other climate modelling codes. The current literature provides some benchmarks of other climate models running the Held-Suarez model configuration, however these studies have been performed on vastly different hardware from that used in this thesis, and therefore cannot be used for a direct comparison of the model [64]. Further work could compare the runtime of other climate models such as the Unified Model on the same hardware as used in this project.

11.3.3 Software architecture

Although this research project focussed solely on porting and optimising the Isca climate model, working on the code for an extended period of time has revealed some shortcomings of the software architecture. The Python wrapper used to run the model and handle data collection is used only as a scripting language to repeatedly run a Fortran executable. This means that multiple versions of the same model configuration cannot exist concurrently, as only one executable can exist for a single model configuration at any time. A more user-friendly design would be to encapsulate the entire model in a Python program, replacing the main Fortran entry point with a Python script. This script would makes calls to Fortran routines using F2PY, instead of just using Python as a scripting language to run the model [96]. This may sacrifice some performance, however many Python libraries are now written in compiled languages like C, C++ or Fortran, and offer the performance benefits of these languages whilst retaining the usability of Python. This change to the codebase would allow for greater customisation of model configurations, as well as allowing for multiple concurrent versions of the model to exist at the same time.

11.3.4 Model configurations

Although the Grey-Mars and Held-Suarez model configurations are vastly different, they only represent two narrow use-cases of the Isca model. Isca can be used for the simulation of countless other scenarios, ranging from the benignly simple to complex realistic global simulations. Further work could look at other use-cases included in the Isca Github repository, including a 'hot Jupiter', 'bucket hydrology' and realistic Earth simulation using topography [11].

11.3.5 Performance projection

As the A64FX processor is currently unreleased, the results from the performance projection cannot be verified. The predictions made in this thesis can be tested in 2021 when the A64FX is released to determine their accuracy.

11.3.6 Catalyst

Hewlett Packard Enterprise in collaboration with Arm, SUSE, and the Universities of Bristol, Edinburgh and Leicester have worked together to produce the Catalyst supercomputer. This machine consists of three identical clusters situated at each university, each consisting of 64 Hewlett Packard Apollo 70 systems, containing two 32 core Cavium ThunderX2 processors. As Isca has demonstrated compelling performance on the Isambard supercomputer, it could be ported to and run on Catalyst.

Bibliography

[1]   G. K. Vallis et al. "Isca, v1.0: a framework for the global modelling of the atmospheres of Earth and other planets at varying levels of complexity". In: *Geoscientific Model Development* 11.3 (Oct. 2018), pp. 843–859. DOI: 10.5194/gmd-11-843-2018.

[2]   E. Calore, F. Mantovani, and D. Ruiz. "Advanced performance analysis of HPC workloads on Cavium ThunderX". In: *2018 International Conference on High Performance Computing & Simulation (HPCS)*. IEEE. July 2018, pp. 375–382. DOI: 10.1109/HPCS.2018.00068.

[3]   S. McIntosh-Smith et al. "A performance analysis of the first generation of HPC-optimized Arm processors". In: *Concurrency and Computation: Practice and Experience* (May 2018), e5110. DOI: 10.1002/cpe.5110.

[4]   N. Okimoto et al. "High-performance drug discovery: computational screening by combining docking and molecular dynamics simulations". In: *PLoS computational biology* 5.10 (2009), e1000528. DOI: 10.1371/journal.pcbi.1000528.t001.

[5]   N. P. Jouppi et al. "In-datacenter performance analysis of a tensor processing unit". In: *2017 ACM/IEEE 44th Annual International Symposium on Computer Architecture*. IEEE. 2017, pp. 1–12. DOI: 10.1145/3079856.3080246.

[6]   C. Bretherton et al. *A national strategy for advancing climate modeling*. 2012. DOI: 10.17226/13430.

[7]   K. Asanovic et al. *The Landscape of Parallel Computing Research: A View from Berkeley*. Tech. rep. UCB/EECS-2006-183. Berkley CA, USA: EECS Department, University of California, Dec. 2006.

[8]   D. J. Becker et al. "BEOWULF: A parallel workstation for scientific computation". In: *Proceedings, International Conference on Parallel Processing*. Vol. 95. 1995, pp. 11–14.

[9]   D. A. Reed. "Beowulf Clusters: From Research Curiosity to Exascale". In: *Proceedings of the 20 Years of Beowulf Workshop on Honor of Thomas Sterling's 65th Birthday*. Annapolis MD, USA, Oct. 2015, pp. 28–33. DOI: 10.1145/2737909.2737913.

[10]   J. P. Evans, M. Ekström, and F. Ji. "Evaluating the performance of a WRF physics ensemble over South-East Australia". In: *Climate Dynamics* 39.6 (2012), pp. 1241–1258. DOI: 10.1007/s00382-011-1244-5.

[11]   Execlim. *Isca: Idealized GCM from the University of Exeter*. Dec. 2018. URL: https://github.com/ExeClim/Isca.

[12]   J. Penn and G. K. Vallis. "The thermal phase curve offset on tidally and nontidally locked exoplanets: A shallow water model". In: *The Astrophysical Journal* 842.2 (2017), p. 101. DOI: 10.3847/1538-4357/aa756e.

[13]   S. I. Thomson and G. K. Vallis. "Atmospheric response to SST anomalies. Part I: Background-state dependence, teleconnections, and local effects in winter". In: *Journal of the Atmospheric Sciences* 75.12 (2018), pp. 4107–4124. DOI: 10.1175/JAS-D-17-0297.1.

[14]   R. Geen, F. Lambert, and G. Vallis. "Regime change behavior during Asian monsoon onset". In: *Journal of Climate* 31.8 (2018), pp. 3327–3348. DOI: 10.1175/JCLI-D-17-0118.1.

[15]   V. Balaji. *The FMS Manual: A developer's guide to the GFDL Flexible Modeling System*. Tech. rep. Princeton, NJ, USA, 2002.

[16]   L. J. Donner et al. "The dynamical core, physical parameterizations, and basic simulation characteristics of the atmospheric component AM3 of the GFDL global coupled model CM3". In: *Journal of Climate* 24.13 (July 2011), pp. 3484–3519. DOI: 10.1175/2011JCLI3955.1.

[17]   R. Farneti and G. K. Vallis. "An Intermediate Complexity Climate Model (ICCMp1) based on the GFDL flexible modelling system". In: *Geoscientific Model Development* 2.2 (July 2009), pp. 73–88. DOI: 10.5194/gmd-2-73-2009.

[18] GFDL. *Flexible Modeling System (FMS)*. July 2019. URL: https://www.gfdl.noaa.gov/fms/.

[19] V. Bjerknes, J. W. Sandstrom, and O. D. Devik. *Dynamic meteorology and hydrography*. 88. Carnegie, 1910.

[20] P. N. Edwards. "History of climate modeling". In: *Wiley Interdisciplinary Reviews: Climate Change* 2.1 (Dec. 2011), pp. 128–139. DOI: 10.1002/wcc.95.

[21] C. L. Godske and V. Bjerknes. *Dynamic meteorology and weather forecasting*. Vol. 605. American Meteorological Society, 1957. DOI: 10.1002/qj.49708335818.

[22] S. McIntosh-Smith et al. "On the performance portability of structured grid codes on many-core computer architectures". In: *International Supercomputing Conference*. Springer. Leipzig ,Germany, June 2014, pp. 53–75. DOI: 10.1007/978-3-319-07518-1_4.

[23] W. Bourke. "Spectral methods in global climate and weather prediction models". In: *Physically-Based Modelling and Simulation of Climate and Climatic Change*. Springer, 1988, pp. 169–220. DOI: 10.1007/978-94-009-3041-4_4.

[24] S. A. Orszag. "Fourier series on spheres". In: *Monthly Weather Review* 102.1 (1974), pp. 56–75. DOI: 10.1175/1520-0493(1974)102<0056\%3AFSOS>2.0.CO\%3B2.

[25] B. Geerts. *Coordinate systems of numerical weather prediction models*. Apr. 1998. URL: http://www-das.uwyo.edu/~geerts/cwx/notes/chap15/coord.html.

[26] H. Goosse et al. *Introduction to climate dynamics and climate modeling*. Centre de recherche sur la Terre et le climat Georges Lemaître-UCLouvain, 2010. URL: http://www.climate.be/textbook.

[27] P. Colella et al. "Performance and scaling of locally-structured grid methods for partial differential equations". In: *Journal of Physics: Conference Series*. Vol. 78. 1. IOP Publishing. June 2007, p. 012013. DOI: 10.1088/1742-6596/78/1/012013.

[28] D. C. Bader et al. "Climate models: an assessment of strengths and limitations". In: (2008). URL: https://digitalcommons.unl.edu/cgi/viewcontent.cgi?article=1009&context=usdoepub.

[29] R. Singleton. "A method for computing the fast Fourier transform with auxiliary memory and limited high-speed storage". In: *IEEE Transactions on Audio and Electroacoustics* 15.2 (1967), pp. 91–98. DOI: 10.1109/TAU.1967.1161906.

[30] J. W. Cooley and J. W. Tukey. "An algorithm for the machine calculation of complex Fourier series". In: *Mathematics of computation* 19.90 (1965), pp. 297–301. DOI: 10.1090/S0025-5718-1965-0178586-1.

[31] H. V. Sorensen et al. "Real-valued fast Fourier transform algorithms". In: *IEEE Transactions on acoustics, speech, and signal processing* 35.6 (1987), pp. 849–863. DOI: 10.1109/TASSP.1987.1165220.

[32] M. Frigo and S. G. Johnson. "FFTW: An adaptive software architecture for the FFT". In: *Proceedings of the 1998 IEEE International Conference on Acoustics, Speech and Signal Processing, ICASSP'98 (Cat. No. 98CH36181)*. Vol. 3. IEEE. 1998, pp. 1381–1384. DOI: 10.1109/ICASSP.1998.681704.

[33] M. Frigo and S. G. Johnson. "The design and implementation of FFTW3". In: *Proceedings of the IEEE* 93.2 (2005), pp. 216–231. DOI: 10.1109/JPROC.2004.840301.

[34] M. Frigo, S. G. Johnson, et al. "FFTW for version 3.3.8". In: (May 2018).

[35] M. T. Heideman, D. H. Johnson, and C. S. Burrus. "Gauss and the history of the fast Fourier transform". In: *Archive for history of exact sciences* 34.3 (1985), pp. 265–277. DOI: 10.1007/BF00348431.

[36] W. M. Gentleman and G. Sande. "Fast Fourier Transforms: for fun and profit". In: *Proceedings of the November 7-10, 1966, fall joint computer conference*. ACM. 1966, pp. 563–578. DOI: 1464291.1464352.

[37] Message Passing Interface Forum. *MPI: A Message-Passing Interface StandardVersion 3.1*. Tech. rep. Knoxville, TN, USA, 2015.

[38]   R. Rew and G. Davis. "NetCDF: an interface for scientific data access". In: *IEEE computer graphics and applications* 10.4 (1990), pp. 76–82. DOI: 10.1109/38.56302.

[39]   R. B. Schmunk. "Panoply netcdf, hdf and grib data viewer". In: *National Aeronautics and Space Administration-Goddard Institute for Space Studies* (2015).

[40]   S. Van Der Walt, S. C. Colbert, and G. Varoquaux. "The NumPy array: a structure for efficient numerical computation". In: *Computing in Science & Engineering* 13.2 (2011), p. 22. DOI: 10.1109/MCSE.2011.37.

[41]   A. Moffat. *sh: a full-fledged subprocess replacement for Python*. June 2017. URL: https://pypi.org/project/sh/.

[42]   A. Ronacher. *Jinja2 Documentation*. Sept. 2017. URL: https://buildmedia.readthedocs.org/media/pdf/jinja2/latest/jinja2.pdf.

[43]   M. L. Ward. *f90nml-A Python module for Fortran namelists*. June 2019. URL: https://pypi.org/project/f90nml/.

[44]   M. J. Flynn. "Some computer organizations and their effectiveness". In: *IEEE transactions on computers* 100.9 (1972), pp. 948–960. DOI: 10.1109/TC.1972.5009071.

[45]   N. Rajovic et al. "Supercomputing with Commodity CPUs: Are Mobile SoCs Ready for HPC?" In: *Proceedings of the International Conference on High Performance Computing, Networking, Storage and Analysis*. SC '13. Denver, Colorado: ACM, Nov. 2013, pp. 41–53. ISBN: 978-1-4503-2378-9. DOI: 10.1145/2503210.2503281.

[46]   G. Conte, S. Tommesani, and F. Zanichelli. "The long and winding road to high-performance image processing with MMX/SSE". In: *Proceedings Fifth IEEE International Workshop on Computer Architectures for Machine Perception*. IEEE. Sept. 2000, pp. 302–310. DOI: 10.1109/CAMP.2000.875989.

[47]   C. Lomont. *Introduction to Intel Advanced Vector Extensions*. Tech. rep. Santa Clara, CA, USA, 2011.

[48]   Intel Corporation. *Intel Architecture Instruction Set Extensions and Future Features Programming Reference*. Tech. rep. Santa Clara, CA, USA, Apr. 2019.

[49]   Intel Corporation. *Intel Xeon Processor E5-2680 v4 product specification*. Jan. 2019. URL: https://ark.intel.com/content/www/us/en/ark/products/91754/intel-xeon-processor-e5-2680-v4-35m-cache-2-40-ghz.html.

[50]   M. Gottschlag and F. Bellosa. "Mechanism to Mitigate AVX-Induced Frequency Reduction". In: *arXiv preprint arXiv:1901.04982* (2018). URL: https://arxiv.org/abs/1901.04982.

[51]   K. Bergman et al. *Exascale computing study: Technology challenges in achieving exascale systems*. Tech. rep. Arlington, VA, USA, 2008.

[52]   Arm Holdings. *Case study: GW4 Alliance puts Arm architecture to the test for HPC*. Tech. rep. Cambridge, United Kingdom, 2018.

[53]   Cavium. *ThunderX2 CN99XX Product Brief*. Tech. rep. San Jose, CA, USA, 2018.

[54]   V. Kindratenko and P. Trancoso. "Trends in high-performance computing". In: *Computing in Science & Engineering* 13.3 (Apr. 2011), p. 92. DOI: 10.1109/MCSE.2011.52.

[55]   N. Rajovic et al. "The Mont-blanc Prototype: An Alternative Approach for HPC Systems". In: *Proceedings of the International Conference for High Performance Computing, Networking, Storage and Analysis*. SC '16. Salt Lake City, Utah: IEEE Press, 2016, pp. 38–50. ISBN: 978-1-4673-8815-3. DOI: 10.1109/SC.2016.37.

[56]   N. Stephens et al. "The ARM scalable vector extension". In: *IEEE Micro* 37.2 (Apr. 2017), pp. 26–39. DOI: 10.1109/MM.2017.35.

[57]   A. Rico et al. "ARM HPC Ecosystem and the Reemergence of Vectors". In: *Proceedings of the Computing Frontiers Conference*. ACM. Sienna, Italy: ACM, May 2017, pp. 329–334. DOI: 10.1145/3075564.3095086.

[58]   G. E. Moore et al. "Cramming more components onto integrated circuits". In: *Electronics* 38.8 (Apr. 1965), pp. 33–35. DOI: 10.1109/N-SSC.2006.4785860.

[59] J. D. McCalpin et al. "Memory bandwidth and machine balance in current high performance computers". In: *IEEE computer society technical committee on computer architecture (TCCA) newsletter* 2.19–25 (Dec. 1995).

[60] D. Patterson et al. "A case for intelligent RAM". In: *IEEE micro* 17.2 (Apr. 1997), pp. 34–44. DOI: 10.1109/40.592312.

[61] J. Hammond. *STREAM memory-bandwidth benchmark*. July 2019. URL: https://github.com/jeffhammond/STREAM.

[62] A. Petitet et al. "HPL - a Portable Implementation of the High-Performance Linpack Benchmark for Distributed-Memory Computers". In: (Jan. 2008).

[63] V. P. Kumar and A. Gupta. "Analyzing scalability of parallel algorithms and architectures". In: *Journal of parallel and distributed computing* 22.3 (1994), pp. 379–391. DOI: 10.1006/jpdc.1994.1099.

[64] M. Schmidt. "A benchmark for the parallel code used in FMS and MOM-4". In: *Ocean Modelling* 17.1 (Dec. 2007), pp. 49–67. DOI: 10.1016/j.ocemod.2006.11.002.

[65] S. Williams, A. Waterman, and D. Patterson. "Roofline: An insightful visual performance model for floating-point programs and multicore architectures". In: *Communications of the ACM - A Direct Path to Dependable Software* 52.4 (Apr. 2009), pp. 65–76. DOI: 10.1145/1498765.1498785.

[66] American National Standard Programming. *Fortran 90 ISO/IEC 1539 : 1991*. Carnegie, 1991.

[67] GNU Project. *Implicit conversion between logical and integer*. July 2019. URL: https://gnu.huihoo.org/gcc/gcc-4.0.4/gfortran/Implicitly-interconvert-LOGICAL-and-INTEGER.html.

[68] D. Goldberg. "What every computer scientist should know about floating-point arithmetic". In: *ACM Computing Surveys (CSUR)* 23.1 (1991), pp. 5–48. DOI: 10.1145/103162.103163.

[69] IEEE Computer Society. Standards Committee and American National Standards Institute. *IEEE standard for binary floating-point arithmetic*. Vol. 754. IEEE, 1985.

[70] M. Johnson and G. Williams. *Program to compare any variables common to two NetCDF files*. June 2009. URL: https://puma.nerc.ac.uk/svn/UniCiCles_svn/UniCiCles/trunk/glimmer-cism/utils/.

[71] I. M. Held and M. J. Suarez. "A proposal for the intercomparison of the dynamical cores of atmospheric general circulation models". In: *Bulletin of the american Meteorological society* 75.10 (1994), pp. 1825–1830. DOI: 10.1175/1520-0477(1994)075<1825:APFTIO>2.0.CO;2.

[72] H. Wan, M. A. Giorgetta, and L. Bonaventura. "Ensemble Held-Suarez test with a spectral transform model: Variability, sensitivity, and convergence". In: *Monthly Weather Review* 136.3 (2008), pp. 1075–1092. DOI: 10.1175/2007MWR2044.1.

[73] P. D. Düben and T. Palmer. "Benchmark tests for numerical weather forecasts on inexact hardware". In: *Monthly Weather Review* 142.10 (2014), pp. 3809–3829. DOI: 10.1175/MWR-D-14-00110.1.

[74] M. Taylor, R. Loft, and J. Tribbia. "Performance of a spectral element atmospheric model (SEAM) on the HP Exemplar SPP2000". In: *NCAR TN* 439 (1998). DOI: 10.5065/D6PR7SX0.

[75] J. Laskar and P. Robutel. "The chaotic obliquity of the planets". In: *Nature* 361.6413 (1993), p. 608. DOI: 10.1038/361608a0.

[76] I. T. Foster and B. R. Toonen. "Load-balancing algorithms for climate models". In: *Proceedings of IEEE Scalable High Performance Computing Conference*. IEEE. July 1994, pp. 674–681. DOI: 10.1109/SHPCC.1994.296706.

[77] J. H. Meeus. *Astronomical algorithms*. Willmann-Bell, Incorporated, 1991.

[78] G. Lancaster. *A collection of scripts for automating runtime and trace data collection for the Isca climate model*. Aug. 2019. URL: https://github.com/Lancasterg/benchmark_isca.

[79] X. Guo et al. *Best Practice Guide - ARM64*. Tech. rep. Germany, 2019.

[80] K. Milfeld. *Parallel Optimization for HPC*. Tech. rep. Austin, TX, USA, 2014.

[81] P. Grun. *Introduction to InfiniBand*. Tech. rep. Santa Clara, CA, USA, 2010.

[82] J. Reinders. *Intel AVX-512 Instructions*. July 2013. URL: https://software.intel.com/en-us/articles/intel-avx-512-instructions.

[83] Intel Corporation. *Intel Architecture Instruction Set Extensions and Future Features Programming Reference*. Tech. rep. Santa Clara, CA, USA, May 2019.

[84] S. Behling et al. *The POWER4 processor introduction and tuning guide*. Tech. rep. Armonk, NY, USA, 2001.

[85] C. Carvalho. "The gap between processor and memory speeds". In: *Proc. of IEEE International Conference on Control and Automation*. 2002.

[86] C. Temperton. "Very Fast Real Fourier Transform". In: *Special topics of applied mathematics: Functional Analysis, Numerical Analysis and Optimisation* (Jan. 1980).

[87] S. Siemen. *Routines for Fast-Fourier Transform (FFT)*. Sept. 2015. URL: https://confluence.ecmwf.int/display/EMOS/FFT+-+FFT991.

[88] T. M. Lahey and T. Ellis. *Fortran 90 programming*. Addison-Wesley Longman Publishing Co., Inc., 1994.

[89] D. L. Parnas. "On the criteria to be used in decomposing systems into modules". In: *Communications of the ACM* 15.12 (1972), pp. 1053–1058. DOI: 10.1145/361598.361623.

[90] Arm Holdings. "Armv8 instruction set overview". In: *vol. PRD03-GENC-010197* 15.11 (2011).

[91] T. Yoshida. "Fujitsu high performance cpu for the post-k computer". In: *Hot Chips 30 Symposium (HCS), Series Hot Chips*. Vol. 18. 2018. URL: https://www.fujitsu.com/jp/Images/20180821hotchips30.pdf.

[92] M. Bach. *Estimating CPU Performance using Amdahl's Law*. May 2015. URL: https://www.pugetsystems.com/labs/articles/Estimating-CPU-Performance-using-Amdahls-Law-619/.

[93] G. M. Amdahl. "Validity of the single processor approach to achieving large scale computing capabilities". In: *Proceedings of the April 18-20, 1967, spring joint computer conference*. ACM. Apr. 1967, pp. 483–485. DOI: 10.1145/1465482.1465560.

[94] S. McIntosh-Smith et al. "TeaLeaf: a mini-application to enable design-space explorations for iterative sparse linear solvers". In: *2017 IEEE International Conference on Cluster Computing (CLUSTER)*. IEEE. 2017, pp. 842–849. DOI: 10.1109/CLUSTER.2017.105.

[95] A. Mallinson et al. "Cloverleaf: Preparing hydrodynamics codes for exascale". In: *The Cray User Group* 2013 (2013).

[96] P. Peterson. "F2PY: a tool for connecting Fortran and Python programs". In: *International Journal of Computational Science and Engineering* 4.4 (2009), pp. 296–305. DOI: 10.1504/IJCSE.2009.029165.

APPENDIX A

Porting code changes

Appendix A lists some of the code changes made in order to compile and run Isca using the Intel, GNU and Cray compilers.

Isambard

Problem 1

Error

This issue was caused by a variation of the Fortran standard between the Cray, GNU and Intel compilers. GNU and Intel allow for implicit conversion between logical, integer and real variables, but the Cray compiler does not. To resolve this issue, a new macro was defined to set a default value depending on the type of variables it was being used for.

```
ftn-356 crayftn: ERROR MPP_DO_GLOBAL_FIELD2D_L8_3D, File = mpp_do_global_field.
    h, Line = 123, Column = 12    Assignment of a INTEGER expression to a LOGICAL
     variable is not allowed.
```

Fix

If `MPP_TYPE_` is of type integer or real, then

```
#define MPP_DEFAULT_VALUE_ 0
```

If `MPP_TYPE_` is of type complex, then

```
#define MPP_DEFAULT_VALUE_  .false.
```

Error 2

```
ftn-1725 crayftn: ERROR COMPUTE_LC1, File = ../../../lustre/home/br-glancaster/
    Isca/src/atmos_spectral/init/polvani_2007.F90, Line = 356, Column = 26
  Unexpected syntax while parsing the assignment statement : "operand" was
     expected but found "-".
```

Cray Fortran requires brackets around all values denoted as negative, for example

```
Tr = T0 + lapse/(zt**-alpha + z(k)**-alpha)**(1./alpha)
```

becomes

```
Tr = T0 + lapse/(zt** (-alpha) + z(k)** (-alpha))**(1./alpha)
```

Error 3

APPENDIX B

Code listings

Grid to Fourier subroutine

```fortran
subroutine grid_to_fourier_double_2d_fftw(num, leng, lenc, grid, fourier)

integer(kind=4),            intent(in)    :: num
integer(kind=4),            intent(in)    :: leng
real(C_DOUBLE),             intent(in)    :: grid(leng, num)
complex(C_DOUBLE_COMPLEX),  intent(out)   :: fourier(lenc, num)
real                                      :: fact
integer                                   :: i, j

fact = 1.0 / (leng - 1)

do j = 1, num
  do i = 1, leng - 1
    real_input(i) = grid(i,j)
  enddo

  call dfftw_execute_dft_r2c(real_input_pointer, real_input, complex_output)

  do i = 1, lenc
    fourier(i, j) = complex_output(i) * fact
  enddo
enddo
return
end subroutine grid_to_fourier_double_2d_fftw
```

Listing B.1: Code used to perform an FFT using the FFTW library. This subroutine can be found in the new `fftw.F90` module, and transforms a 2D data structure from the spacial domain to frequency domain.

Program to time FFT

```fortran
subroutine time_fft()
use fft_mod

real(kind=8)   , allocatable  :: ain(:,:), aout(:,:)
complex(kind=8), allocatable  :: four(:,:)
integer    :: i, j, m, n, k, h, iter, lot
integer    :: ntrans(3) = (/ 128, 256, 512 /)
integer    :: lots(3) = (/ 64, 128, 256 /)
real       :: start_time = 0, stop_time = 0, mean_time_iter = 0, mean_time_full
    = 0, append_time = 0, time_3d_start = 0, time_3d_stop = 0

iter = 100

! test multiple transform lengths
  do m = 1, 3

  ! set up input data
    n = ntrans(m)
    lot = lots(m)
```

```fortran
19
20     allocate(ain(n+1,lot),aout(n+1,lot),four(n/2+1,lot))
21
22     call fft_init(n)
23
24     do k = 1, iter
25         call random_number(ain(1:n,:))
26         four = fft_grid_to_fourier(ain)
27         call cpu_time(start_time)
28             aout = fft_fourier_to_grid(four)
29         call cpu_time(stop_time)
30         append_time = append_time + (stop_time - start_time)
31     enddo
32
33     mean_time_iter = append_time / iter
34
35     append_time = 0.0
36     start_time = 0.0
37     stop_time = 0.0
38
39     do k = 1, iter
40         call random_number(ain(1:n,:))
41         four = fft_grid_to_fourier(ain)
42         call cpu_time(time_3d_start)
43         do h = 1, 25
44             aout = fft_fourier_to_grid(four)
45         enddo
46         call cpu_time(time_3d_stop)
47         append_time = append_time + (time_3d_stop - time_3d_start)
48     enddo
49
50     mean_time_full = append_time / iter
51
52     call fft_end()
53     deallocate (ain,aout,four)
54
55     print *, '( ',n,' x ' ,lot ,' ), mean_iteration_time: '
56     write (*,'(f15.9)') mean_time_iter
57     print *, '( ',n,' x ' ,lot ,' ), mean_full_time: '
58     write (*,'(f15.9)') mean_time_full
59  enddo
60
61 end subroutine time_fft
62
63 end program test
```

APPENDIX C

Compile environment scripts

Isambard GNU

```
1  # template for the  gfortran compiler
2  # typical use with mkmf
3  # mkmf -t template.ifc -c"-Duse_libMPI -Duse_netCDF" path_names /usr/local/
       include
4  CPPFLAGS = -I/usr/local/include
5  NETCDF_LIBS = `nf-config --fflags  --flibs`
6
7  # FFLAGS:
8  #  -cpp: Use the fortran preprocessor
9  #  -ffree-line-length-none -fno-range-check: Allow arbitrarily long lines
10 #  -fcray-pointer: Cray pointers don't alias other variables.
11 #  -ftz: Denormal numbers are flushed to zero.
12 #  -assume byterecl: Specifies the units for the OPEN statement as bytes.
13 #  -shared-intel:  Load intel libraries dynamically
14 #  -i4: 4 byte integers
15 #  -fdefault-real-8: 8 byte reals (compatability for some parts of GFDL code)
16 #  -fdefault-double-8: 8 byte doubles (compat. with RRTM)
17 #  -O2: Level 2 speed optimisations
18
19 FFLAGS = $(CPPFLAGS) $(NETCDF_LIBS) -cpp -fcray-pointer \
20          -O2 -ffree-line-length-none -fno-range-check \
21          -fbacktrace -target-cpu=arm-thunderx2 -fdefault-real-8 -fdefault-
    double-8
22
23 #        -ftree-vectorize -fopt-info-vec-missed
24
25 #FFLAGS = $(CPPFLAGS) $(NETCDF_LIBS) -cpp -fcray-pointer \
26 #         -O2 -ffree-line-length-none -fno-range-check \
27 #         -fdefault-real-8 -fdefault-double-8 -fbacktrace \
28 #           -target-cpu=arm-thunderx2
29
30 FC = $(F90)
31 LD = $(F90) $(NETCDF_LIBS)
32
33 LDFLAGS = -lnetcdff -lnetcdf
34 CFLAGS = -D__IFC
```

BCP3 Intel

```
1  # template for the Intel fortran compiler
2  # typical use with mkmf
3  # mkmf -t template.ifc -c"-Duse_libMPI -Duse_netCDF" path_names /usr/local/
       include
4  CPPFLAGS = -I/usr/local/include
5  NETCDF_LIBS = `nc-config --libs`
6
7  # FFLAGS:
8  #  -fpp: Use the fortran preprocessor
9  #  -stack_temps:  Put temporary runtime arrays on the stack, not heap.
10 #  -safe_cray_ptr: Cray pointers don't alias other variables.
```

```
11 #   -ftz: Denormal numbers are flushed to zero.
12 #   -assume byterecl: Specifies the units for the OPEN statement as bytes.
13 #   -shared-intel:  Load intel libraries dynamically
14 #   -i4: 4 byte integers
15 #   -r8: 8 byte reals
16 #   -g: Generate symbolic debugging info in code
17 #   -O2: Level 2 speed optimisations
18 #   -diag-disable 6843:
19 #       This suppresses the warning: 'warning #6843: A dummy argument with an
     explicit INTENT(OUT) declaration is not given an explicit value.' of which
20 #       there are a lot of instances in the GFDL codebase.
21 FFLAGS = $(CPPFLAGS) -fpp -stack_temps -safe_cray_ptr -ftz -assume byterecl -
     shared-intel -i4 -r8 -g -O2 -diag-disable 6843
22 #FFLAGS = $(CPPFLAGS) -fltconsistency -stack_temps -safe_cray_ptr -ftz -shared-
     intel -assume byterecl -g -O0 -i4 -r8 -check -warn -warn noerrors -debug
     variable_locations -inline_debug_info -traceback
23 FC = $(F90)
24 LD = $(F90) $(NETCDF_LIBS)
25 #CC = mpicc
26
27 LDFLAGS = -lnetcdff -lnetcdf -lmpi -shared-intel
28 CFLAGS = -D__IFC
```

APPENDIX D

Job submission scripts

BCP3 (PBS)

```
1  #!/bin/sh
2
3  #PBS -n held_suarez_benchmarking
4  #PBS -V # export all environment variables to the batch job.
5  #PBS -d . # set working directory to .
6  #PBS -q long # submit to the long queue
7  #PBS -l nodes=1:ppn=16
8  #PBS -l walltime=72:00:00 # Maximum wall time for the
9  #PBS -m e -M qv18258@bristol.ac.uk
10
11 source activate isca_env
12 python $BENCHMARK_ISCA/src/main.py -codebase grey_mars -mincores 4 -maxcores 4
      -r T21 -r T42 -r T85
```

BluePebble (PBS Pro)

```
1  #!/bin/sh
2  #PBS -l select=1:ncpus=28:mem=20GB
3  #PBS -l walltime=72:00:00
4
5  module load tools/git/2.22.0
6  source activate isca_env
7  python $BENCHMARK_ISCA/src/main.py -mincores 16 -maxcores 16 -r T21 -r T42 -
      codebase grey_mars -fc kind_4
```

Isambard (PBS Pro)

```
1  #!/bin/sh
2
3  #PBS -q arm
4  #PBS -l select=1:ncpus=64
5  #PBS -l walltime=23:00:00
6  #PBS -M =qv18258@bristol.ac.uk
7
8  source ~/isca_env/bin/activate
9  python $BENCHMARK_ISCA/src/main.py -mincores 4 -maxcores 4 -r T21 -r T42 -r T85
       -codebase held_suarez -fc cray_temp
```

BCP4 (SLURM)

```
1  #!/bin/Bash
2
3  #SBATCH --job-name=benchmark_held_suarez_two_cores
4  #SBATCH --partition=cpu
5  #SBATCH --time=4-00:00:00
6  #SBATCH --nodes=1
7  #SBATCH --ntasks-per-node=24
8  #number of cpus (cores) per task (process)
```

```
 9 #SBATCH --cpus-per-task=1
10 #SBATCH --output=held_suarez_two_cores_%j.o
11 #SBATCH --mail-type=ALL
12 #SBATCH --mail-user=qv18258@bristol.ac.uk
13
14 echo Running on host `hostname`
15 echo Time is `date`
16 echo Directory is `pwd`
17
18 module purge
19 source $HOME/.Bashrc
20 source $GFDL_BASE/src/extra/env/bristol-bc4
21 source activate isca_env
22
23 $HOME/.conda/envs/isca_env/bin/python $BENCHMARK_ISCA/src/main.py -mincores 2 -
       maxcores 2 -r T21 -r T42 -codebase held_suarez -fc gcc
```